

KfK 2847
September 1979

Calibration of Neutron Detectors in Radiation Protection

**A Report on the Karlsruhe Results of the
European Neutron Dosimetry
Intercomparison Program 1977/78**

**E. Piesch, B. Burgkhardt, I. Hofmann
Hauptabteilung Sicherheit**

Kernforschungszentrum Karlsruhe

KERNFORSCHUNGSZENTRUM KARLSRUHE

Hauptabteilung Sicherheit

KfK 2847

CALIBRATION OF NEUTRON DETECTORS IN RADIATION PROTECTION

A Report on the Karlsruhe Results of the European
Neutron Dosimetry Intercomparison Program 1977/78

E. Piesch, B. Burgkhardt, I. Hofmann

Kernforschungszentrum Karlsruhe GmbH, Karlsruhe

Als Manuskript vervielfältigt
Für diesen Bericht behalten wir uns alle Rechte vor

Kernforschungszentrum Karlsruhe GmbH
ISSN 0303-4003

Abstract

During the European Intercomparison Experiment at the PTB Braunschweig and GSF Neuherberg in 1977/78 neutron dosimeters have been calibrated with monoenergetic neutrons in the energy range 19 MeV down to 2 keV as well as with Am-Be, ^{252}Cf and thermal neutrons.

The report presents the final results above all the energy dependence found for our instrumentation

- rem counters which are of the Studsvik type, a 30 cm diam. polyethylene sphere with a BF_3 -counter in the center and a 25 cm diam. sphere with TLD 600/TLD 700 in the center
- a passive spectrometer with TLD 600/TLD 700 detectors along the axis of a cylinder
- a special albedo counter with three BF_3 -counters,
- the Karlsruhe albedo neutron dosimeter system
- Kodak NTA film
- fission fragment track detectors applying ^{237}Np and ^{232}Th
- recoil track detector using Kodak LR-115
- recoil track detector using Makrofol and electrochemical etching.

For moderator type detectors in addition scanning profiles for the n_{th} , 2 keV and 25 keV reactor beam neutrons are presented. On the basis of the experiments, the calibration technique applied in albedo dosimetry is improved to interpret neutron stray radiation fields.

KALIBRIERUNG VON NEUTRONENDETEKTOREN FÜR DEN STRAHLENSCHUTZ

Ein Bericht über die Karlsruher Ergebnisse des Europäischen Neutronendosimetrie-Vergleichsprogrammes 1977/78

Zusammenfassung

Innerhalb der Europäischen Vergleichsbestrahlungen bei der PTB Braunschweig und der GSF Neuherberg in den Jahren 1977/78 wurden Neutronendosimeter mit monoenergetischen Neutronen im Energiebereich 19 MeV bis 2 keV sowie mit Am-Be, ^{252}Cf und thermischen Neutronen kalibriert.

Der Bericht gibt die endgültigen Ergebnisse wieder, die vor allem für die Energieabhängigkeit unserer Meßgeräte erhalten wurden:

- Rem-Zähler vom Typ Studsvik, eine 30 cm \emptyset Polyäthylen-Kugel mit einem BF_3 -Zählrohr im Zentrum und eine 25 cm \emptyset Kugel mit TLD 600/TLD 700 im Zentrum,
- ein passives Spektrometer mit TLD 600/TLD 700 Detektoren entlang der Zylinderachse,
- das Karlsruher Albedoneutronendosimetersystem,
- der Kodak NTA Film
- die Spaltfragment-Kernspurdetektoren mit ^{237}Np und ^{232}Th ,
- Rückstoßkernspurdetektoren mit Makrofol und einer elektrochemischen Ätztechnik.

Für die Reaktorbeam-Bestrahlungen mit n_{th} , 2 keV und 24 keV werden zusätzlich Scanning-Profile wiedergegeben. Aufgrund der experimentellen Ergebnisse wird die in der Albedodosimetrie angewandte Kalibriertechnik verbessert, um auch Neutronenstreustrahlungsfelder zu interpretieren.

<u>Contents</u>	<u>page</u>
1. Introduction	1
2. Calibration	1
3. Energy dependence of neutron monitors	6
3.1 Passive Spectrometer	6
3.2 Rem counter	11
3.3 Albedo counter	13
4. Energy dependence of personnel dosimeters	14
4.1 Albedo dosimeter	14
4.2 Fission track detectors	20
4.3 Recoil track detectors	23
4.4 NTA film	25
4.5 Gamma dosimeter	25
5. Scanning profile of moderator type detectors	27
5.1 Detector in center	27
5.2 Detector on the surface	29
5.3 Detector along the beam axis	31
6. Interpretation of neutron spectra	33
7. References	37

1. Introduction

The European Radioprotection Dosimeter Intercomparison Program of the last years offered the opportunity to calibrate personnel dosimeters in a wide neutron energy range and to investigate neutron detectors for an application in personnel monitoring and neutron dosimetry. In 1977, teams from several European countries participated in four experiment sessions at the Physikalisch-Technische Bundesanstalt (PTB).

In the years 1977 - 1978, an additional intercomparison exposure was organized at the Gesellschaft für Strahlen- und Umweltforschung (GSF), Neuherberg.

The Karlsruhe Nuclear Research Center took part in this European Intercomparison Program with various neutron detectors recently developed in our laboratory. In the report the final results of our experiments are presented discussing above all the response vs. energy characteristic of rem counters, albedo dosimeters, track etch detectors as well as moderator type devices which may be applied to interpret neutron spectra in terms of effective neutron energy. The results of these experiments are the basis for the introduction of new calibration techniques and the routine application of new developed detector types.

2. Calibration

During the European Intercomparison Experiments the PTB offered the following neutron standard fields:

- a thermal neutron beam from the 1-MW-Research Reactor,
- filtered 2 keV and 24 keV neutron beams from the reactor,
- neutrons from ^{252}Cf and Am-Be (α, n) sources,
- neutrons produced by a 3.75 MeV Van de Graaf accelerator in the range between 100 keV and 19 MeV.

Table 1: Neutron filter and beam properties

Energy	2 keV	24.5 keV
Beam tube	S5, tangential	S4, radial
Main filter	708 mm Sc, dia. 57 mm	352 mm Fe, dia. 40 mm
Additional filter	15 mm Ti	230 mm Al, 75 mm S
Resonance scatterer	10 mm Mn powder (resonance at 2.38 keV)	---
Difference filter	25 mm Mn powder	5 mm Ti
At irradiation position:		
beam diameter	13.5 cm	8.5 cm
neutron current density in the centre of the beam ^{*)}	$1600 \text{ cm}^{-2} \text{ s}^{-1}$	$2200 \text{ cm}^{-2} \text{ s}^{-1}$
Neutron current ^{*)}	$2.4 \cdot 10^5 \text{ s}^{-1}$	$1.3 \cdot 10^5 \text{ s}^{-1}$
Portion of neutrons with energies above the main filter energy ^{*)}	$\sim 1.2 \%$	$\sim 15 \%$
max. gamma dose equivalent rate in soft tissue ^{*)}	25 nWkg^{-1}	3 nWkg^{-1}

^{*)} Values for the difference beams at 1 MW reactor power

Table 2: Data for the neutron reference fields.

These are given for a distance of 1 m at 0° to the incoming beam. For the energy of 100 keV an angle of 30° was taken. The maximum dose equivalent rate was calculated according to ICRP Publication 21 /4/.

Reaction	Neutron energy	Neutron current density	Neutron maximum dose equivalent rate	Gamma dose equivalent rate in soft tissue
	MeV	$\text{cm}^{-2} \cdot \text{s}^{-1}$	Wkg^{-1}	Wkg^{-1}
$^{45}\text{Sc}(p,n)^{45}\text{Ti}$	0.050	$0.02 \cdot 10^3$	$0.006 \cdot 10^{-7}$	
$^7\text{Li}(p,n)^7\text{Be}$	0.100	$2.8 \cdot 10^3$	$1.7 \cdot 10^{-7}$	$8 \cdot 10^{-9}$
$^7\text{Li}(p,n)^7\text{Be}$	0.250	$4.0 \cdot 10^3$	$5.6 \cdot 10^{-7}$	$27 \cdot 10^{-9}$
$^7\text{Li}(p,n)^7\text{Be}$	0.570	$52 \cdot 10^3$	$111 \cdot 10^{-7}$	$93 \cdot 10^{-9}$
$\text{T}(p,n)^3\text{He}$	1.000	$6 \cdot 10^3$	$20 \cdot 10^{-7}$	$8 \cdot 10^{-9}$
$\text{T}(p,n)^3\text{He}$	2.500	$30 \cdot 10^3$	$120 \cdot 10^{-7}$	$58 \cdot 10^{-9}$
$\text{D}(d,n)^3\text{He}$	5.00	$18 \cdot 10^3$	$74 \cdot 10^{-7}$	$140 \cdot 10^{-9}$
$\text{T}(d,n)^4\text{He}$	15.5	$18 \cdot 10^3$	$75 \cdot 10^{-7}$	$4 \cdot 10^{-9}$
$\text{T}(d,n)^4\text{He}$	19.0	$4 \cdot 10^3$	$17 \cdot 10^{-7}$	$35 \cdot 10^{-9}$

Table 3: Fluence to dose equivalent conversion factors after [6] according to ICRP Recommendation 21

E (MeV)	h_{Φ} (J/kg)·cm
$2.5 \cdot 10^{-8}$	$1.068 \cdot 10^{-11}$
$2.0 \cdot 10^{-3}$	$0.98 \cdot 10^{-11}$
$2.45 \cdot 10^{-2}$	$1.85 \cdot 10^{-11}$
$1.0 \cdot 10^{-1}$	$5.78_2 \cdot 10^{-11}$
$2.5 \cdot 10^{-1}$	$1.18 \cdot 10^{-10}$
$5.7 \cdot 10^{-1}$	$2.18 \cdot 10^{-10}$
1.0	$3.26_8 \cdot 10^{-10}$
2.5	$4.01 \cdot 10^{-10}$
5.0	$4.08_5 \cdot 10^{-10}$
15.5	$4.18 \cdot 10^{-10}$
19.0	$4.22 \cdot 10^{-10}$

Table 4: Basic data for GSF irradiation after [4]

reaction	particle energy (MeV)	mean neutron energy (MeV)	fluence to kerma conversion factor (10^{-9} rad)	fluence to dose equivalent conversion factor (10^{-8} rem cm ²)
T(p,n)He ³	1.50	0.57	1.71	2.22
T(p,n)He ³	2.90	2.07	3.09	4.00
T(d,n)He ⁴	0.40	15.1	6.70	4.08
D(d,n)He ³	2.30	5.25	4.49	4.00
Cf-fission neutrons	--	--	--	3.3
AmBe neutrons	--	--	--	3.6

Characteristic data about the filtered neutron beams and the neutron fields at the accelerator are presented in Tables 1 and 2 [1].

The neutron dose equivalent was calculated on the basis of fluence to dose equivalent conversion factors (Table 3). Due to the actual situation at the thermal beam, the effective energy of thermal neutrons was taken as 65 meV which results in a conversion factor of $1.11 \cdot 10^{-11}$ J cm²/kg for thermal neutrons. The neutron fluence results are measured in the beam free in air at the place of calibration. For the beam calibration of the accelerator a proton recoil proportional counter [2] and a proton recoil telescope [3] are used.

The response R of a neutron detector was determined by the ratio

$$R = \frac{\text{instrument reading}}{\text{value of the reference quantity causing the instrument reading}}$$

At the GSF neutron irradiations have been performed with a 3 MeV Van de Graaff generator and with ²⁵²Cf and Am-Be (α,n) (Table 4) [4]. For beam monitoring a tissue equivalent ionization chamber at 50 mm distance from the target is used. The reference quantity is the Kerma in soft tissue at 30 cm source distance free in air on the beam axis determined absolutely during an International Intercomparison [5].

The irradiations at the PTB have been performed in a distance in the range of 1 m to 3 m between the source center (accelerator target) and the center of the dosimeter or for phantom irradiation the front surface of the phantom. The phantoms used were water-filled polyethylene cylinders 0.6 m in height and 0.3 m in diameter irradiated perpendicular to the axis of rotation.

For the reactor beam irradiations a scanning technique was applied and the dosimeter or phantom was either scanned step by step along a diameter perpendicular to the beam or over the full cross section of the dosimeter or phantom.

The uncertainties of the fluence determination (one standard deviation) at the PTB is presented in Table 5. These data mainly represent systematic errors of measurement and are not included in the error bars presented in the curves of the figures which are mainly statistic uncertainties of the dose reading.

Table 5: Standard deviation for the calibration exposure at PTB [6]

Neutron Energy keV	Relative Standard Deviation of Fluence Determination	Neutron Energy keV	Relative Standard Deviation of Fluence Determination
2	16 %	1000	5 %
24,5	12 %	2500	5-6 %
100	6-8 %	5000	5-6 %
250	6-12 %	15500	5-9 %
570	5-8 %	19000	12 %
		rad. sources	5%

The influence of a neutron background on the dosimeter indication was generally not taken into account. This effect is proportional to the energy dependence of the dosimeter response. For accelerator irradiations the background scattered neutrons (<5%) can be neglected. During the experiment an additional contribution of lower energy neutrons from the target was found at 19 MeV which was determined to be about 10% for the Leake type rem counter [29] (see also chapter 6). Only at 2 keV the dosimeter response results of moderating spheres were reduced by a factor 0.5 to correct for beam neutrons of higher energies.

Compared to calibration of the Leake type rem counter recently done with a Sb/Be source at Harwell about 20% higher results have been found at the PTB for the response at 24 keV [31]. Uncertainties may arise primarily from the potential existence of low-energy neutron in the 24 keV beams whose presence cannot be determined by the proton-recoil spectroscopy applied at the PTB.

More information about the standard neutron fields, the technique of calibration and exposure as well as the estimation of measuring uncertainties are described in additional reports which summarize also most of the final results of the participants [6].

Our laboratory participated with the following instrumentation:

- Rem counter type Studsvik 2202 D.
- Moderating spheres 30 cm in diameter containing BF_3 detector.
- Spectrometer-Dosimeter. Cylindrical moderator diam. 25 cm, length 25 cm, irradiated "end-on" (side on at 24 keV). Results taken from a TLD 12 cm inside the moderator. No scanning at the filtered beam of 2 keV.
- Albedo counter. Polyethylene cylinder with 3 BF_3 tubes (special development, KFK Karlsruhe); results obtained from "detector i". At 2 keV only scanned without difference filter.
- Karlsruhe Albedo dosimeter system; results obtained from "detector i".
- Track etch fission fragment detector with ^{237}Np .
- Track etch fission fragment detector with ^{232}Th .
- Kodak NTA film.
- Red dyed recoil track detector, Kodak LR-115.
- Makrofol recoil track detector, electrochemical etching.
- Phosphate glass dosimeter.

3. Energy Dependence of Neutron Monitors

3.1 Passive Spectrometer

The neutron spectrometer used in this experiment consists of a 25 cm diameter and 25 cm long polyethylene cylinder containing pairs of TLD 600 and TLD 700 detectors along the axis of the cylinder positioned in equidistance intervals of 0.8 cm (Fig. 1).

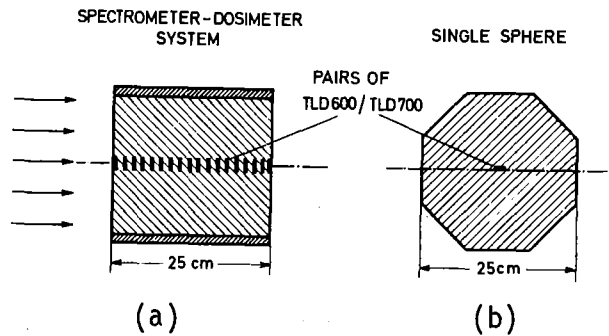


Fig. 1 Cross section of the neutron spectrometer (a) and the dosimeter (b) with cylindrical shape

The polyethylene cylinder is covered with a cadmium shield except for the front face of the cylinder where the radiation beam is incident.

The depth dose distribution of TLD 600 readings in beam direction along the cylinder axis was investigated after subtraction of the gamma dose fraction by means of the TLD 700 reading. The gamma equivalent neutron reading of TLD 600 which was obtained in such a way is plotted against the depth in the polyethylene cylinder and represents mainly the thermal fluence distribution.

The response characteristic of the detector has been investigated recently in the radiation field of Pu-Be, ^{252}Cf and 14 MeV neutrons taking into account different kinds of shieldings and backscattering conditions [7].

The neutron response of the TLD 600 dosimeters along the beam axis is presented in Figs. 2 and 3 as a function of depth for monoenergetic neutrons in the energy range from n_{th} to 19 MeV. The maximum of the depth dose curve varies with neutron energy and was found in a depth of 1 cm for thermal neutrons up to a depth of 8 cm for 15.5 MeV neutrons. The response vs. depth dose curves differ significantly at the surface and in the maximum resulting in a similar decrease after a depth of 2 cm and 3 cm, respectively.

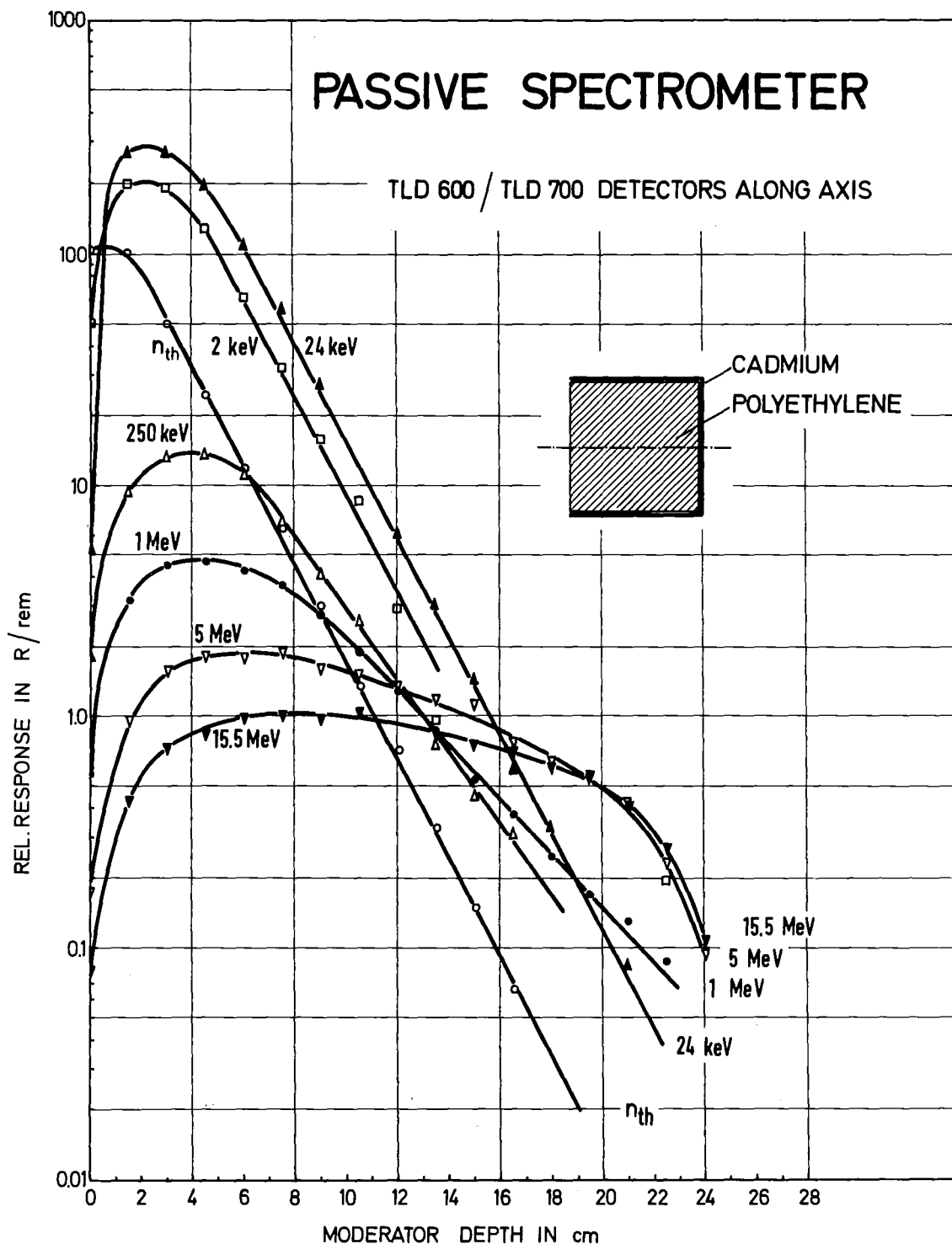


Fig. 2 Gamma equivalent neutron dose reading of TLD 600/TLD 700 dosimeters in Roentgen per neutron dose equivalent of 1 rem as a function of depth in beam axis

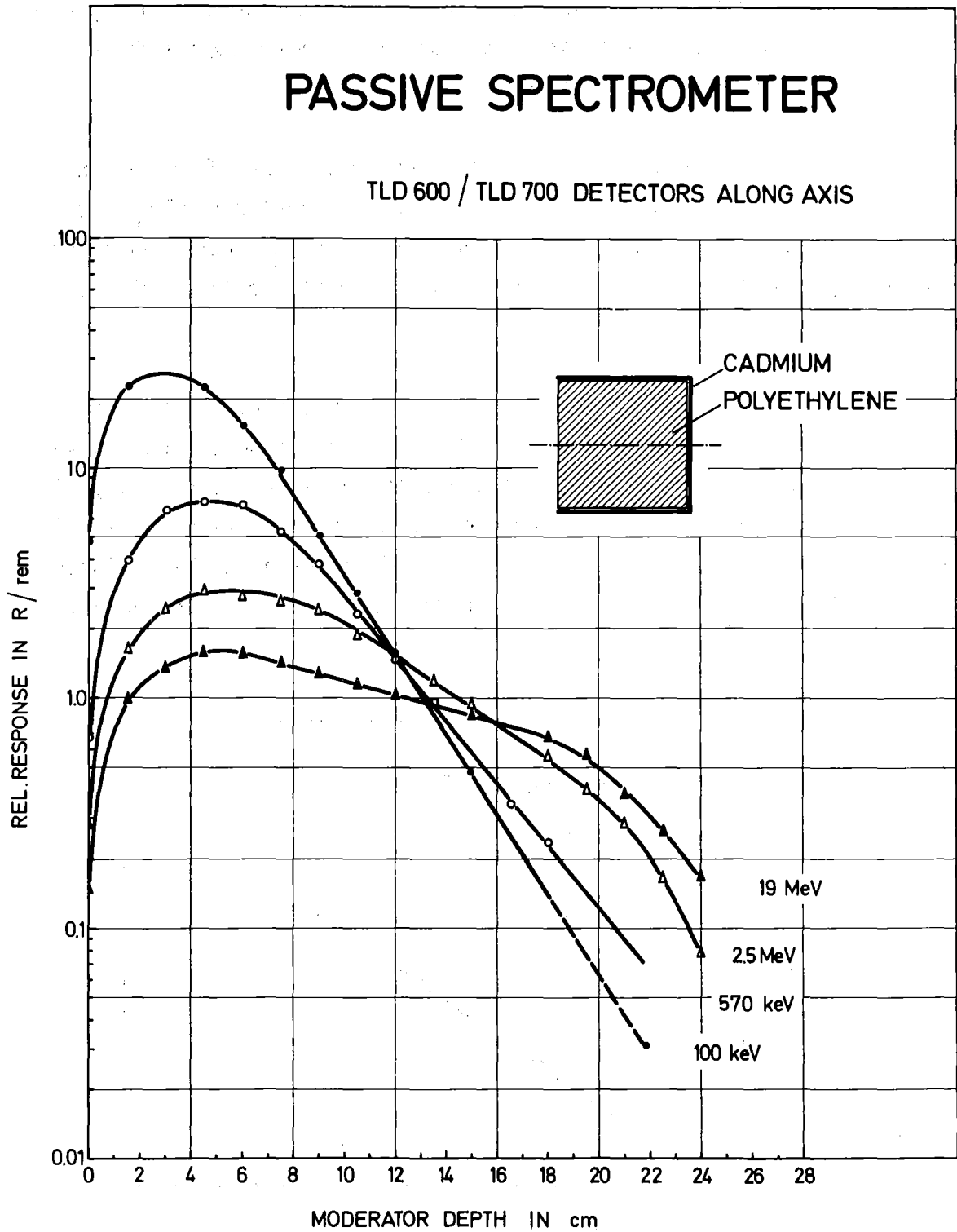


Fig. 3 Neutron response of the passive spectrometer with TLD 600/TLD 700 detectors along the cylinder as a function of depth

The lowest scatter in the response results has been found in a depth of 12 cm, the energy dependence of such a passive rem counter with the detector in 12 cm depth is presented in Fig. 6.

On the basis of the response vs. depth dose curves the effective energy of the neutron spectrum can be estimated. For an analysis of E_{eff} the response in a depth of 12 cm and in the maximum of the depth dose curve can be applied. Fig. 4 shows the response ratio $R(12 \text{ cm})/R(\text{max})$ vs. neutron energy.

In a stray radiation field the effective neutron energy can be estimated only in the energy range 25 keV to 5 MeV because the depth dose curve for 2 keV and 24 keV neutrons are similar in shape and do not vary significantly for neutrons above 5 MeV in the decrease of response in higher depths. In addition the shape of the depth dose curve can be analyzed for an additional interpretation of the neutron spectra (see section 6).

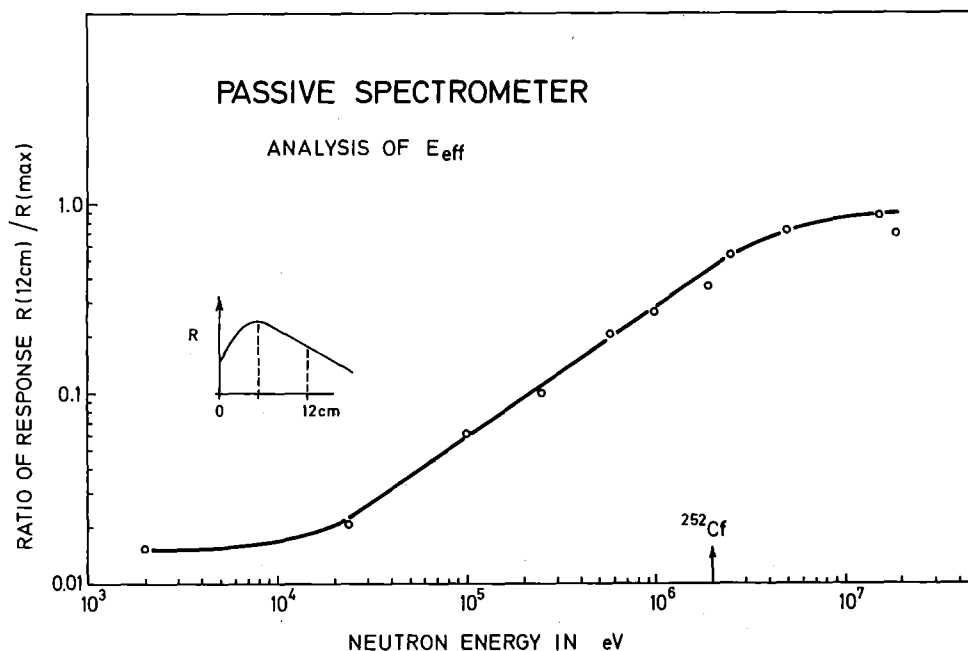


Fig. 4 Ratio of response in 12 cm depth and in the maximum of depth dose curve vs. neutron energy

3.2 Rem Counter

During the Euratom experiment at the PTB in Brunswick the following rem counters have been investigated:

- BF_3 counter in the center of a sphere of 30 cm diameter,
- BF_3 counter in the axis of a cylinder (Studsvik rem counter of the Anderson-Braun type),
- TLD 600/TLD 700 dosimeter pairs in the center of a "single sphere" (cylindrical shape 25 cm in length and diameter, see also Fig. 1),
- TLD 600/TLD 700 dosimeter pairs in the center of the cylinder of 25 cm length and diameter.

In Fig. 5 the response of the rem counter sphere of 30 cm diameter is presented as a function of neutron energy. In the energy range of 10 keV the response was found to be higher by a factor 3 compared to the results at 1 MeV. The rem counter underestimated thermal neutrons with 17%. Compared to the Studsvik rem counter or a passive rem counter (see Fig. 6) there is a significant increase in response which was found to be in the order of 60% for the energy range 1 to 5 MeV. The calibration of the Studsvik rem counter by other investigators resulted in a high energy dependence in the order of a factor 8 [6].

Passive rem counters of 25 cm diameter, on the other hand, may overestimate neutrons in the energy range 1 keV to 20 keV up to a factor 4 and underestimate thermal neutrons significantly (Fig. 6).

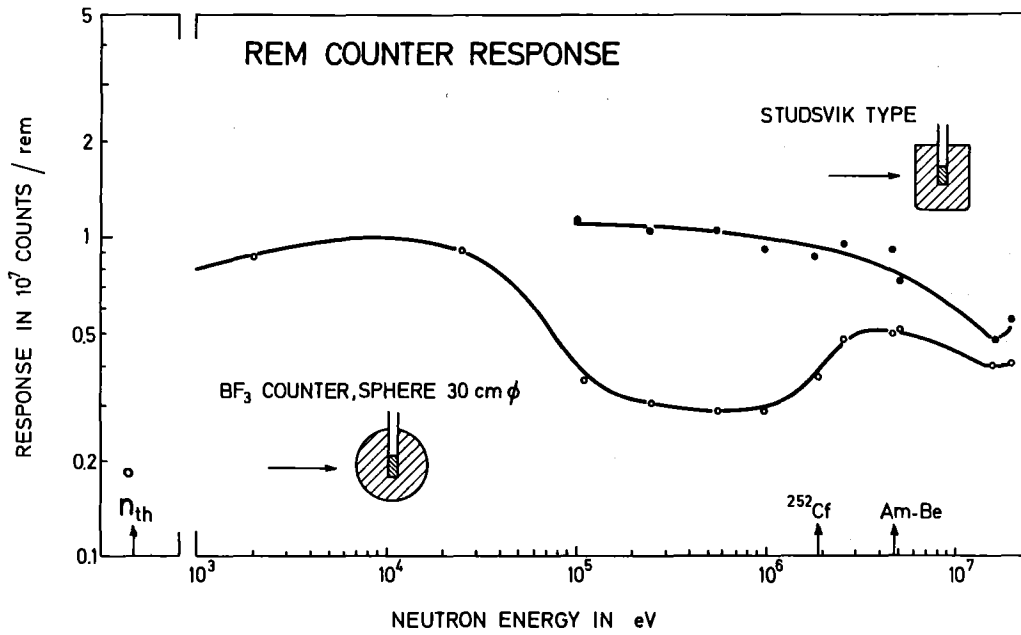


Fig. 5 Response vs. neutron energy for the Studsvik rem counter and a rem counter with a BF₃ counter in the center of a sphere of 30 cm diameter

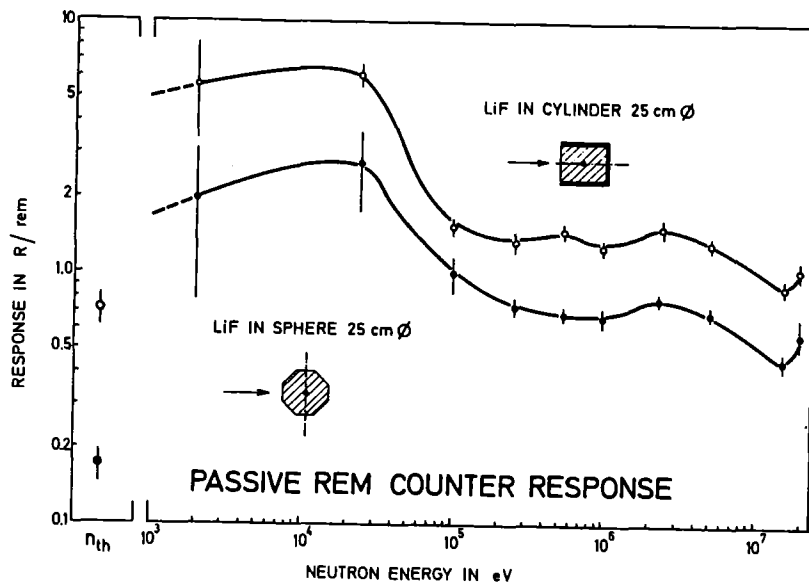


Fig. 6 Response vs. neutron energy for passive rem counters with TLD 600/TLD 700 in the center of a moderator

3.3 Albedo Counter

For an application in albedo dosimetry a so-called albedo counter was designed to simulate the properties of the Karlsruhe albedo neutron dosimeter (see also section 4.1). Instead of TLD 600/TLD 700 detectors the albedo counter makes use of three BF_3 counters which are positioned at the surface of a phantom in the detector positions a, m, i, outside or behind a boron plastic shield [8].

The relative response of the albedo counter is presented in Fig. 7 as a function of neutron energy and compared to the albedo dosimeter results.

In the energy range above 5 MeV the detector characteristic of the albedo counter in position i varies significantly from the results found for the albedo dosimeter. This effect can be explained by the volume of the BF_3 counter which is larger compared to the more or less point size of the TLD detector.

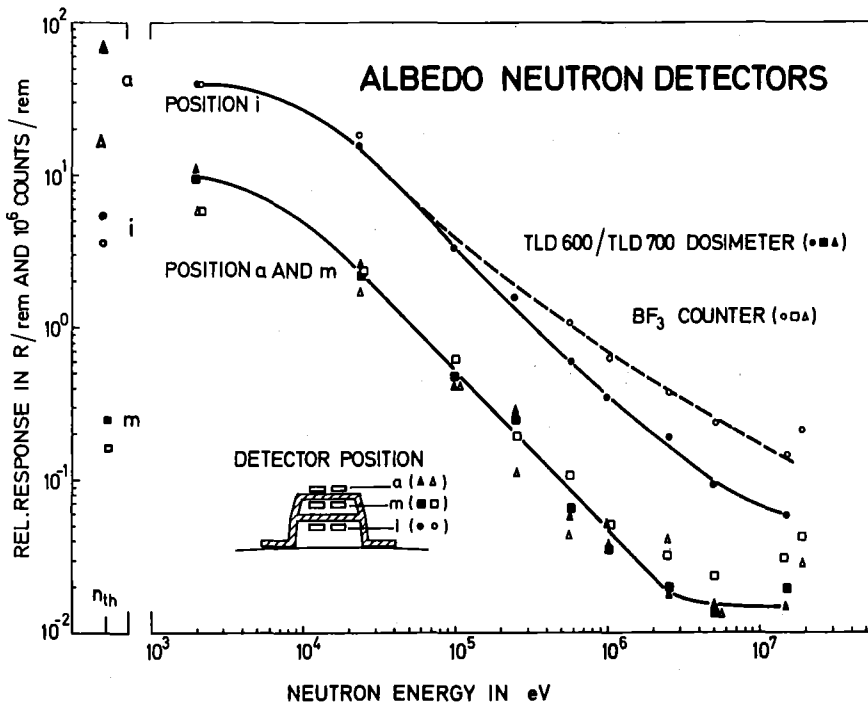


Fig. 7 Response vs. neutron energy of the Karlsruhe albedo dosimeter and an albedo counter with BF_3 detectors

4. Energy Dependence of Personnel Dosimeters

4.1 Albedo Dosimeter

4.1.1 Energy and Direction Dependence

Albedo dosimeters contain one or more pairs of TLD 600/TLD 700 thermoluminescence detectors providing separate indication of incident and backscattered neutrons. For the estimation of the neutron dose equivalent pairs of TLD 600/TLD 700 detectors are used to detect thermal neutrons via the ${}^6\text{Li}(n,\alpha)\text{T}$ reaction and to separate the gamma dose fraction by using the difference in the dosimeter readings.

In the Karlsruhe albedo dosimeter [9-11] three pairs of TLD 600/TLD 700 dosimeters are positioned in a boron plastic capsule (see also Fig. 8). The estimation of the neutron dose equivalent is based only on dosimeter pair i located inside the boron capsule facing the body. The neutron dose equivalent H_n is thus given by

$$H_n = k(i_6 - i_7)$$

Here, i_6 and i_7 are the dosimeter readings of the TLD 600/TLD 700 detector pair in the position i (albedo neutron readings), k is a calibration factor dependent on the neutron energy or on the local neutron spectrum.

In addition, the dosimeter pairs a and m are used to correct for the energy response of the albedo dosimeter i on the basis of calibrations. Local energy correction factors for k can be derived experimentally for each actual neutron spectrum at a given working place.

The so-called albedo dosimeter system consisting of two dosimeters worn by a belt at the front and at the rear of the body serves for an approximately direction-independent indication of the neutron dose equivalent.

Table 6: Energy response of the Karlsruhe Albedo Dosimeter and the albedo counter found for monoenergetic neutrons at the PTB Braunschweig

NEUTRON ENERGY (keV)	DOSIMETER RESPONSE ¹⁾					
	(R/rem)			(1/mrem)		
	ALBEDO DOSIMETER ²⁾			ALBEDO COUNTER ²⁾		
	i	m	a	i	m	a
n _{th}	3.94	0.155	42.5	3700	160	16200
2	26.32	5.30	4.55	40800	5700	5600
24	9.71	1.57	1.55	18100	2200	1700
100	2.08	0.249	0.245	--	560	392
250	0.95	0.18	0.19	--	180	157
570	0.39	0.036	0.034	1048	96.1	43.2
1000	0.20	0.023	0.031	603	37.6	52.4
2500	0.12	0.010	0.012	368	32.4	59.8
5000	0.07	0.007	0.008	231	23.2	13.3
15000	0.03	0.005	0.009	145	31.1	79.3
19000	--	--	--	213	43.1	27.8

¹⁾ Response presented as the ¹³⁷Cs equivalent reading in Roentgen per neutron dose equivalent of 1 rem (TLD) or the count rate per 1 mrem/h (BF₃-counter)

²⁾ Karlsruhe albedo dosimeter with the TLD 600 / TLD 700 pairs or BF₃-counters in the position i (facing the body), a (outside boron) and m (inside boron)

The response of the albedo detector i is presented in Fig. 8 as a function of neutron energy for a frontal irradiation of the albedo dosimeter at the surface of a phantom. In this figure the experimental response which is defined here as a gamma equivalent neutron reading of the detector i in the unit Roentgen found for the neutron dose equivalent of 1 rem is compared with the calculated results from Alsmiller and Barish [12] after normalization at 1 MeV. For the read-out of the thermoluminescent detector two different maximum heating temperatures have been applied to measure glow peak 5 and glow peak 5 and 6, respectively. The reproducibility of dose measurement was found to be higher in the lower dose range of 10 mR to 100 mR if only glow peak 5 is evaluated [13].

The main characteristic of the Karlsruhe albedo dosimeter has been found in the nearly equal response for thermal neutrons and 50 keV neutrons and in a higher response for 2 keV neutrons. Without taking into account the thermal neutron response, the response vs. energy curves are similar for the detector a, m, and i (see Fig. 9) as well as for other albedo dosimeters like the Hoy type [14] or the Hankins type [15]. The results of the calibration exposure demonstrate that the design of an albedo dosimeter type only improve the thermal neutron response and the sensitivity of the dose reading, respectively (see also Table 6).

The response of the albedo detector i has been investigated as a function of neutron energy for three different directions of incidence. Fig. 10 shows the variation in response at the front of a phantom for a side (90°) and a rear (180°) irradiation incidence relative to the response found for a front irradiation.

The results found with monoenergetic neutrons during the Euratom experiment in 1977 at the PTB Brunsvik show a high decrease in the response with decreasing neutron energy. For neutron spectra in stray radiation fields, however, the directional dependence of the rear albedo response at low neutron energies has been found to be smaller by a factor of 10 compared to the results for monoenergetic neutrons depending on the degree of moderation and the fraction of thermal neutrons. Under practical

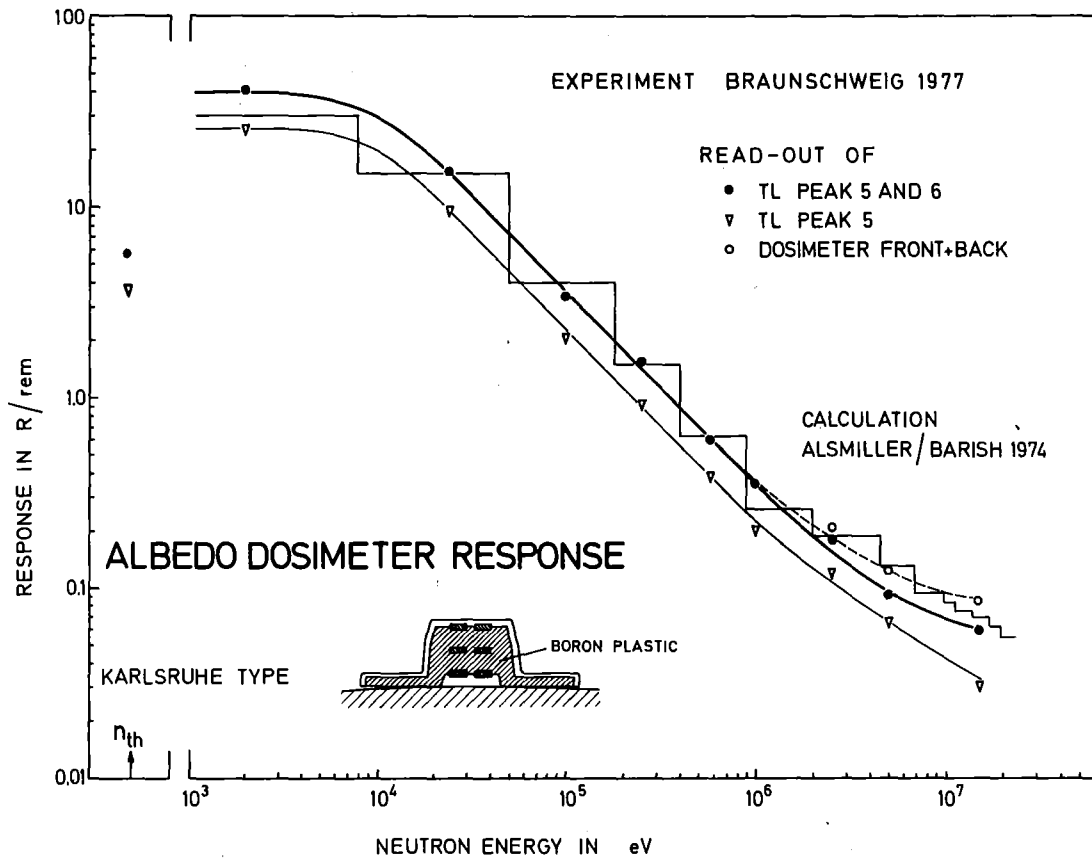


Fig. 8 Energy dependence of the Karlsruhe albedo dosimeter for TLD 600/TLD 700 in position i compared with calculated data

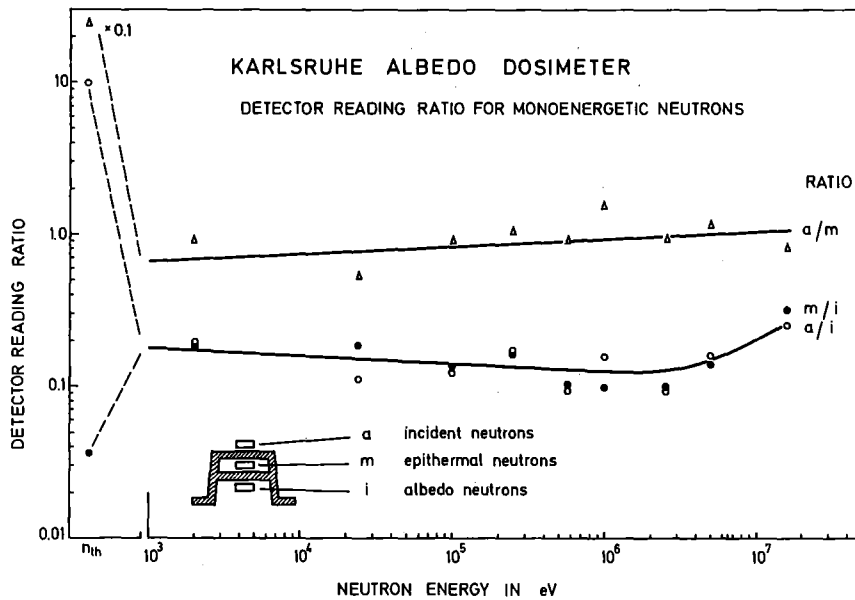


Fig. 9 Detector reading ratio of the Karlsruhe albedo dosimeter vs. neutron energy

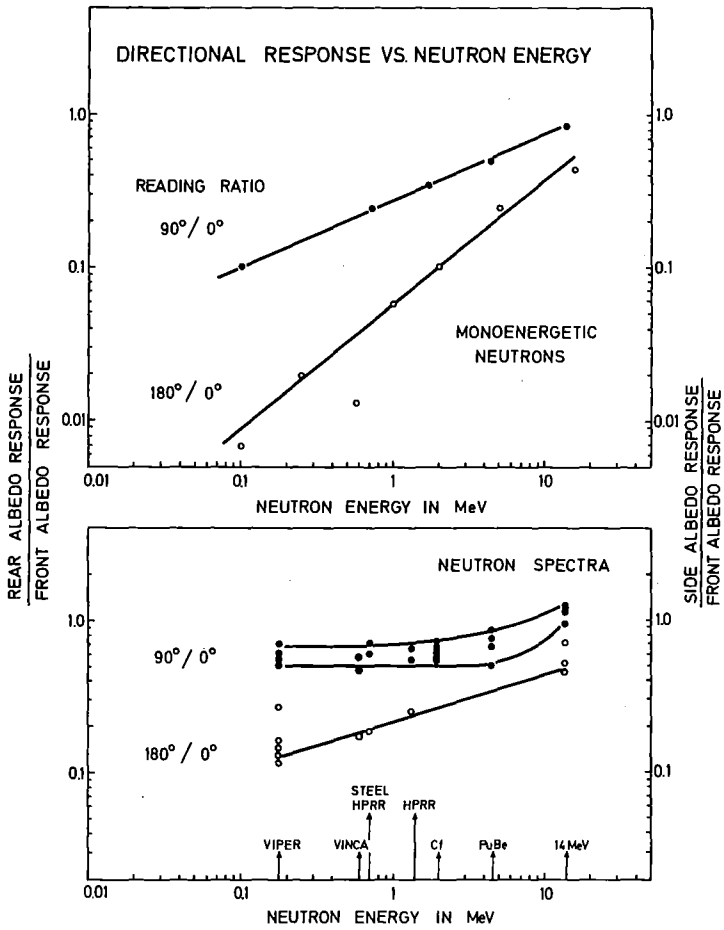


Fig. 10

Directional dependence vs. neutron energy for the Karlsruhe albedo dosimeter

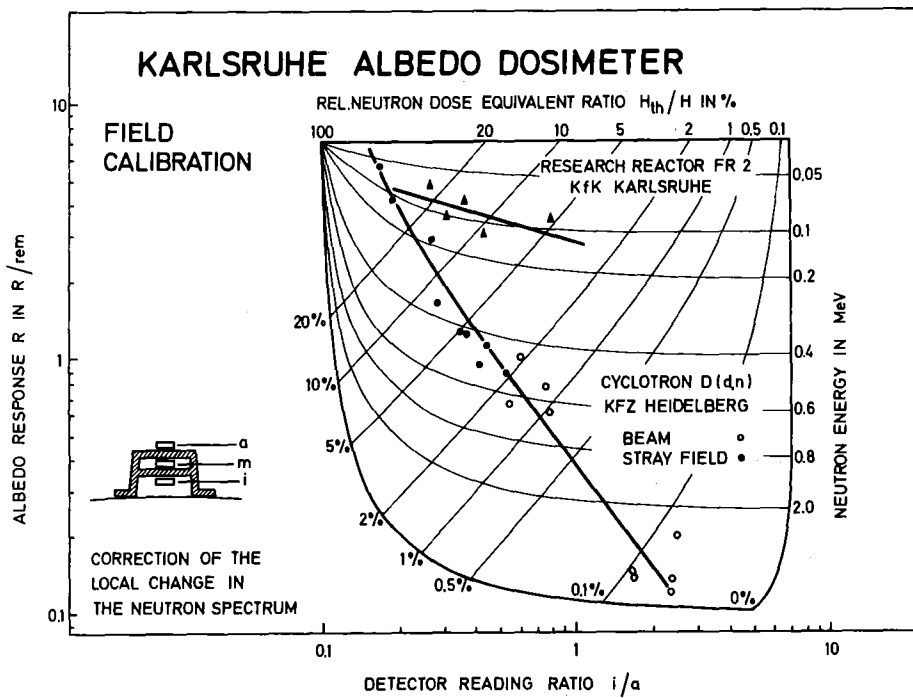


Fig. 11 Response of the albedo detector i as a function of detector ratio i/a with H_{th}/H and E as parameters

field conditions the albedo response decreases in the energy range 15 MeV to 0.01 MeV only down to 15% for radiation incidence at 90° and down to 10% at 180° .

An albedo dosimeter system consisting of two dosimeters at the front and the rear of the body may therefore reduce the direction dependence significantly also in the lower energy range [10].

4.1.2 Interpretation of Dose Reading and/or Neutron Spectra in Stray Radiation Fields

The Karlsruhe albedo dosimeter allows the separate indication of albedo neutrons (detector element i), incident thermal neutrons (detector element a), and epithermal neutrons (detector element m). In Fig. 9 the detector reading ratios are presented as a function of neutron energy. Above 1 keV the results show no significant change of the dose reading ratio vs. neutron energy. A significant change in the dose reading ratio can be applied only for incident thermal neutrons (ratio i/a) or for epithermal neutrons in the eV energy range (ratio a/m).

On the basis of the theoretical assumption that the neutron dose equivalent can be described as a sum of two fractions, the dose equivalent for the effective neutron energy and the dose equivalent fraction of thermal neutrons, the albedo response R can be presented as a function of the detector reading ratio i/a (Fig. 11). For monoenergetic neutrons, of course, no significant change in the detector reading ratio i/a is observed. Depending on the local conditions in the stray radiation field, the albedo response R_{eff} may vary over a range of two decades given by the area presented in Fig. 11. On the basis of field calibrations the spectrum dependent response of the dosimeter reading i can be corrected sufficiently by using the experimental relationship $R_{\text{eff}} = f(i/a)$ which for example is presented in Fig. 11 for two different stray radiation fields. The application of this technique is discussed elsewhere [10, 16, 17].

4.1.3 The Field Calibration

The field calibration of the Karlsruhe albedo dosimeter system is based on the reading of a rem counter of 30 cm diameter and the albedo dosimeter system which both are similar in the directional characteristic. Instead of a field calibration the reading ratio of 9"/3" spheres are applied to simulate the calibration of the albedo dosimeter in stray radiation fields [15], assuming that the energy response curves of the 3" sphere and of the albedo dosimeter are identical and the reading of the 9" sphere rem counter can be interpreted as the dose equivalent at the location of interest.

All moderator techniques, however, have been found to be inaccurate and fail in stray radiation fields with $E_{\text{eff}} < 100$ keV. This is demonstrated in Fig. 12 for calibration techniques applying the reading of an albedo counter or the ratio 9"/3" or 12"/2" spheres. Here in addition the neutron dose equivalent will be overestimated by the energy dependence of the rem counter and the response ratio 2 keV to thermal neutrons vary significantly in a different way for both reference instruments and albedo dosimeter types.

During the European calibration program at the PTB, on the other hand, a significant difference has been found in experimental and calculated data of the sphere ratio 12"/2" [18] (Fig. 13).

4.2 Fission Track Detectors

The fission track detector consists of a Makrofol detector foil of 13 μm thickness in contact with a thick thorium foil or in contact with a ^{237}Np layer electro-plated in a thickness of 40 $\mu\text{g}/\text{cm}^2$ on a steel plate. After applying the conventional etching process the detector foils have been counted in a spark counter after Cross and Tommasino [19].

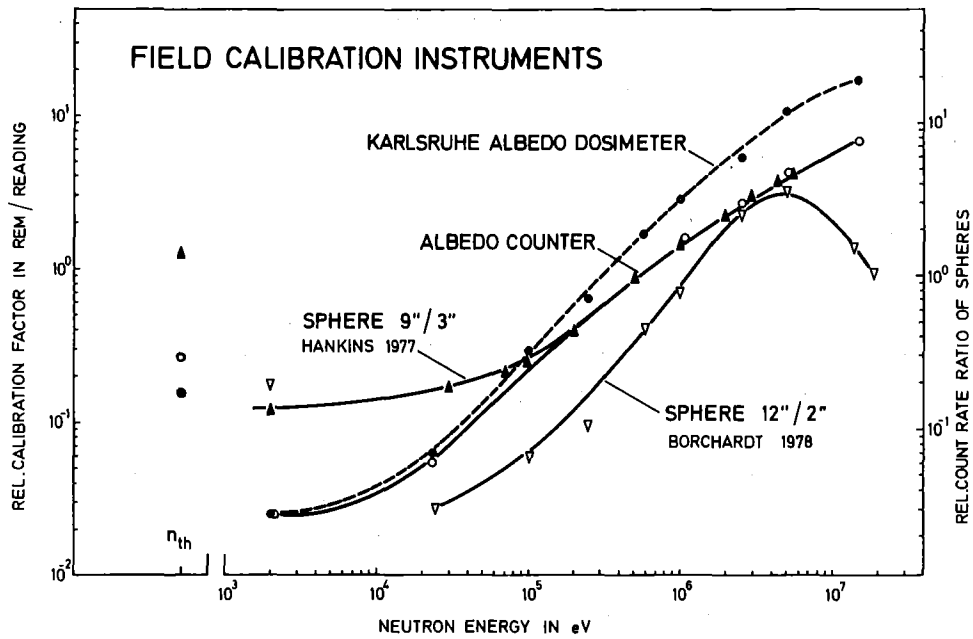


Fig. 12 Calibration factor of albedo detectors compared to the reading ratio 9"/2" and 12"/2" spheres vs. neutron energy

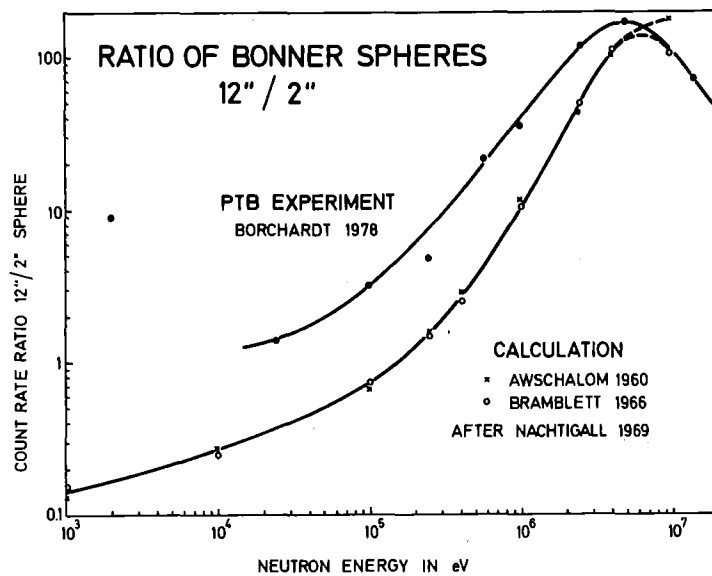


Fig. 13 Comparison of measured and calculated reading ratio of 12"/2" spheres

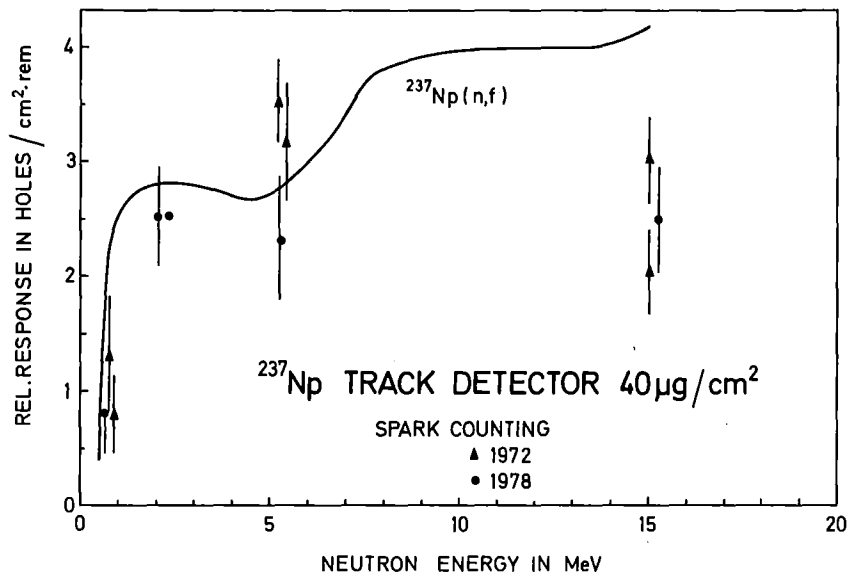


Fig. 14 Energy dependence of ²³⁷Np fission fragment track etch detector vs. neutron energy and the ²³⁷Np (n,f) cross section

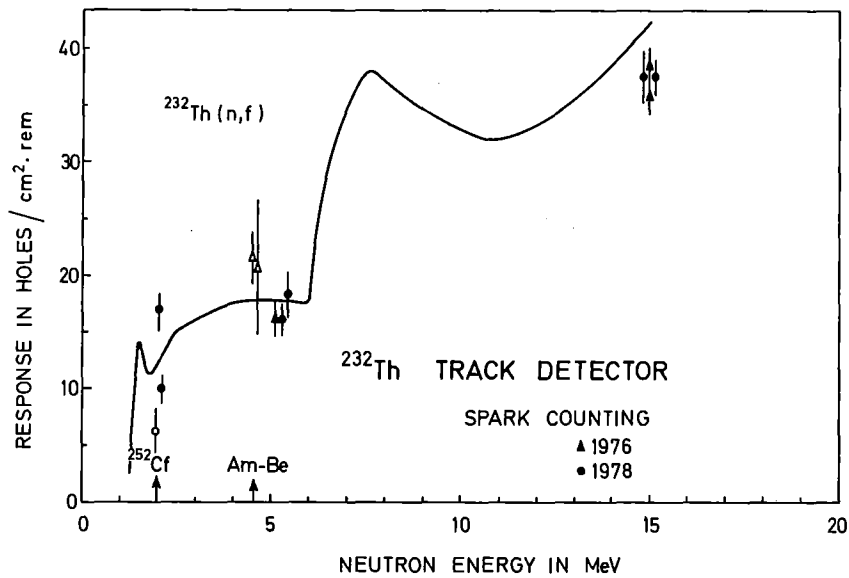


Fig. 15 Energy dependence of ²³²Th fission fragment track etch detector vs. neutron energy and the ²³²Th (n,f) cross section

The energy response of fission track detectors has been investigated during the European Intercomparison Experiment at the GSF in Neuherberg. The response of the ^{237}Np fission fragment detector is presented in Fig. 14 as a function of neutron energy and compared to the cross section curve of the fission reaction. Above the threshold of 0.5 MeV the neptunium detector shows an energy dependence in the order of factor 4. The experimental results for 15 MeV neutrons has been found to be lower compared to the cross section curve.

The experimental results of the thorium fission fragment detector is presented in Fig. 15. The response characteristic is comparable to the cross section curve resulting in an energy dependence of the order of factor 4 to 5 above the threshold of 1.2 MeV. The relatively high standard deviation presented in the figures results mainly from the low sensitivity and/or the low exposure of the dosimeters.

4.3 Recoil Track Etch Detectors

The response vs. energy curve has been investigated for the Kodak LR-115 cellulose nitrate film of different thicknesses by applying two different etching times [20]. The holes which appeared as bright spots in a dark red background were counted using an optical microscope. The response of this recoil track detector (Fig. 16) shows a threshold energy at 1 MeV for the maximum possible etching time and a continuous increase in response which was found to be proportional to the neutron energy.

The most actual technique in personal monitoring today is the detection of neutron induced recoils in Makrofol. After applying an electro-chemical etching process (ECE) the track etch diameters can be extended to more than 150 μm . This technique becomes more and more popular by applying a pre-etching technique which reduces the background level significantly [20, 22]. Fig. 17 shows the response of the recoil track detector as a function of neutron energy for an electro-chemical etching at 1.5 keV

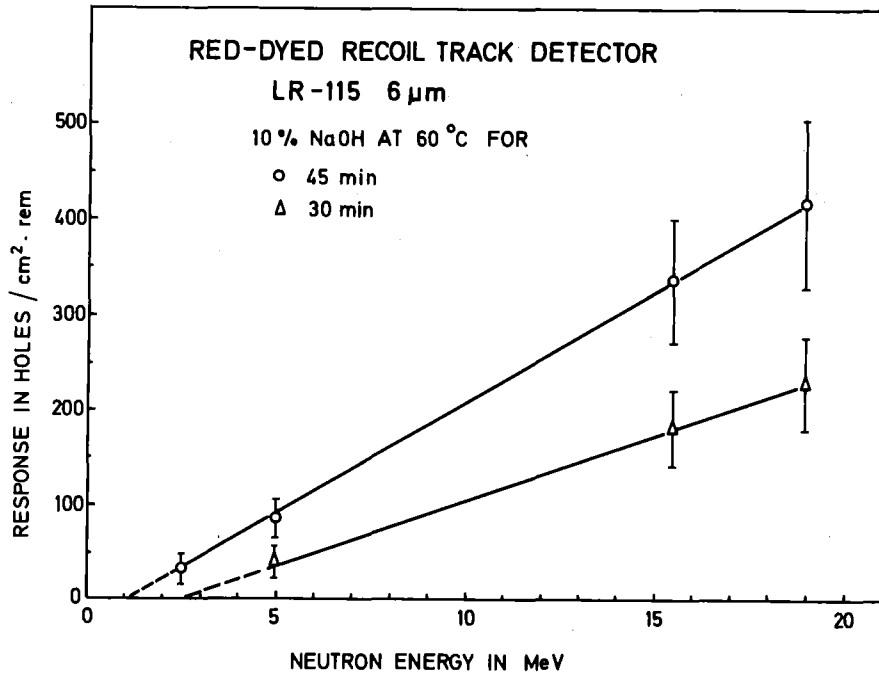


Fig. 16 Response of the Kodak LR-115 film applied as recoil track etch detector vs. neutron energy

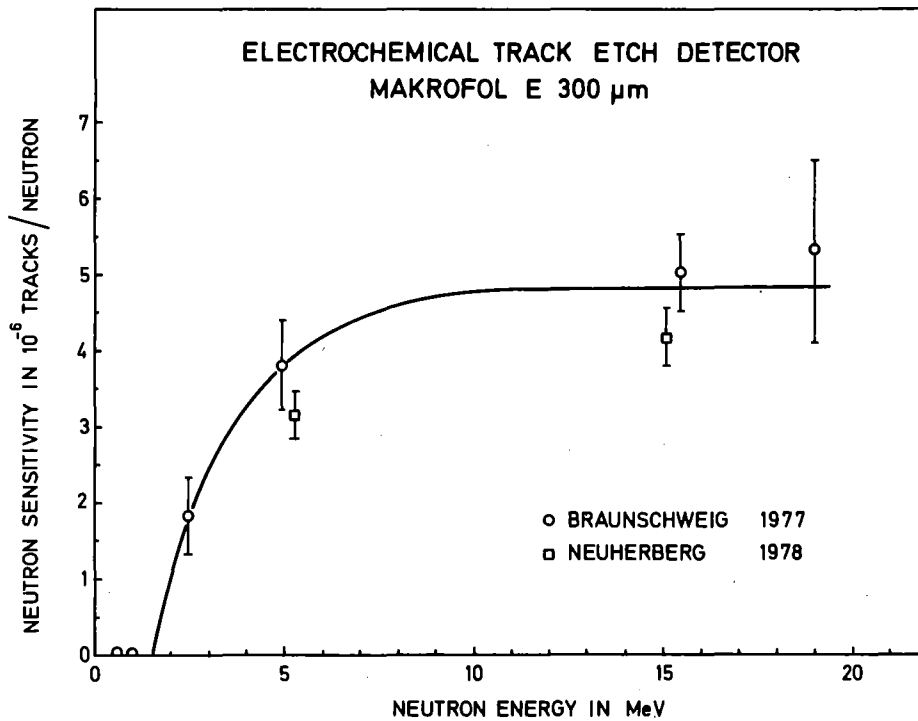


Fig. 17 Response vs. neutron energy, of Makrofol E recoil track etch detector after electrochemical etching

and 500 Hz. With a threshold energy of 1.5 MeV the response increases sharply with neutron energy upto 4 MeV resulting in a fairly constant value upto 19 MeV. These results are in agreement with similar calibrations [23]. For conventional etching, however, a lower threshold energy of 0.8 MeV was reported [24].

4.4 NTA Nuclear Track Film

In Fig. 18 the experimental results of the European Intercomparison Experiment at the GSF is presented for the Kodak NTA film which has been routinely sealed under dry nitrogen atmosphere in an aluminium plastic foil by governmental laboratory service. Compared to the calculated response curve [25] the dosimeter response was found to be in the order of 50% after 14 days of storage (1976) or only 30% after 45 days of storage (1978) at room temperature. These fading results agree with previously reported results in our laboratory [26] but are not compatible with recently published data [27].

For the 1976 Intercomparison Exposure a significant effect on the measured response was observed depending on the kind of irradiation (Fig. 19). Compared to a free air irradiation phantom irradiations resulted in a lower response which is in contrast to all other experimental data indicating an increase in response at the phantom due to backscattered neutrons [25, 28]. The influence of an additional gamma background can be excluded. There is, however, no indication for a fading effect due to the phantom material.

4.5 Gamma Dosimeters

During the PTB experiment also gamma dosimeters have been irradiated free in air to monoenergetic neutrons. The dosimeter reading was corrected for the gamma contribution in the neutron beam given by PTB on the basis of GM-counter measurements (see Tables 1 and 2).

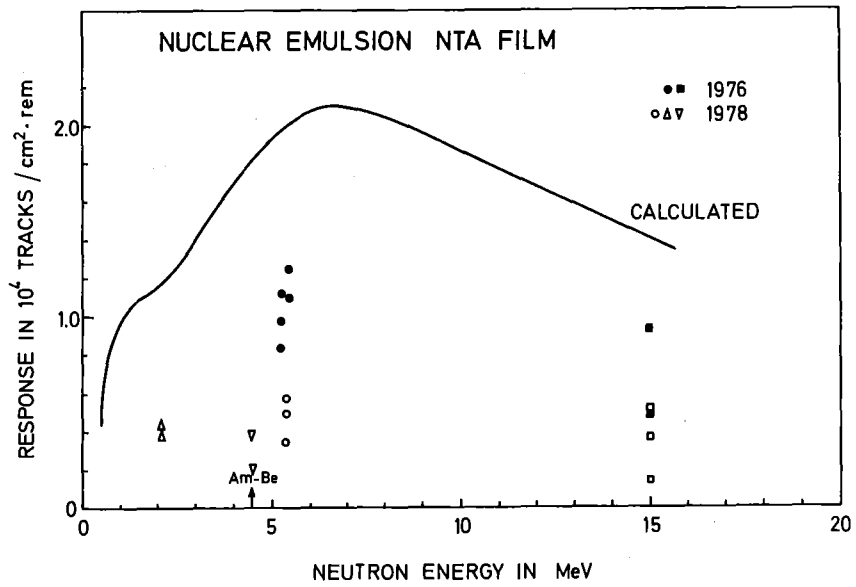


Fig. 18 Measured and calculated response vs. neutron energy of the Kodak NTA film emulsion sealed in aluminium/plastic foil

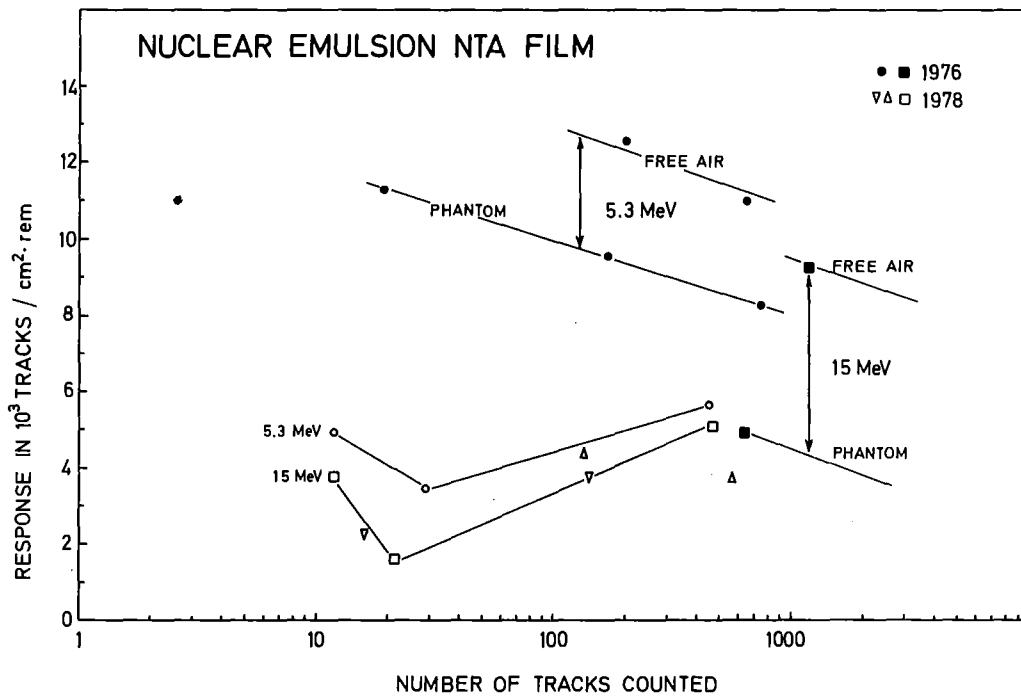


Fig. 19 Response vs. number of tracks of the NTA film for free air and phantom exposures

At the Karlsruhe Nuclear Research Center the phosphate glass dosimeter in the spherical capsule (boron/plastic sphere covered by a perforated tin layer) is the basic personnel dosimeter for routine monitoring of gamma rays and after a criticality accident of thermal and fast neutrons via the activation of phosphorous [30]. This phosphate glass dosimeter is also applied by governmental services as a replace for the film dosimeter. The neutron response of the phosphate glass dosimeter FD-1 given as the gamma equivalent reading in Roentgen is presented in Fig. 20 as a function of neutron energy for the boron/tin sphere as well as for a cadmium and a tin capsule of 1 mm and 1.2 mm thickness, respectively. For an application in personnel monitoring the spherical dosimeter resulted in a nearly equal response for thermal neutrons and gamma rays if an albedo factor of 0.8 will be taken into account. This results are in agreement with former calibrations [30]. Compared to a tin capsule the boron/tin sphere reduces the neutron response by a factor of 10. In the energy range of intermediate neutrons a $1/v$ response was found according to the cross section of ^6Li and ^{10}B . The response for fast neutrons has been found to be low compared to other TLD detectors like LiF.

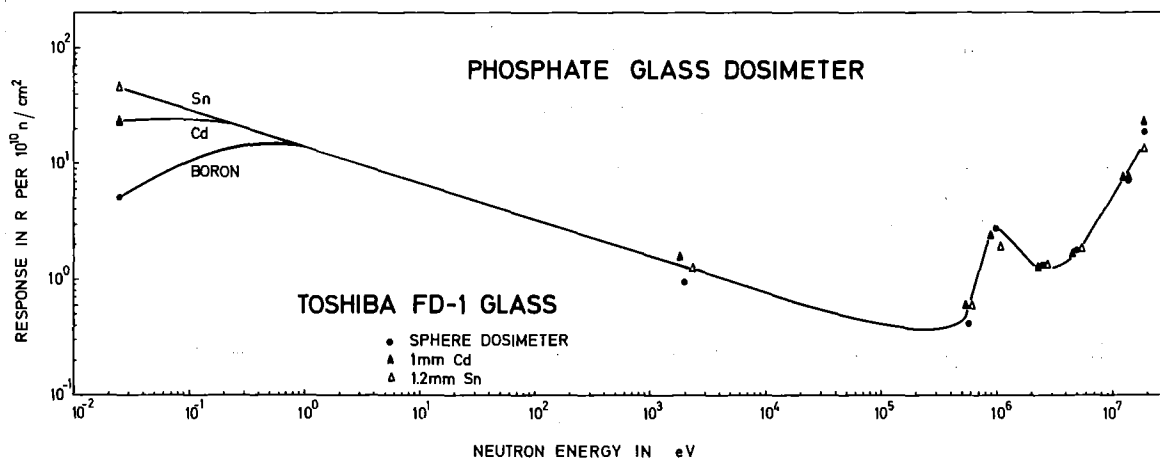


Fig. 20 Energy dependence of phosphate glass dosimeters

5. Scanning Profile of Moderator Type Detectors

5.1 Detector in the Center

The scanning profile was investigated for the BF_3 counter in the center of the polyethylene sphere of 30 cm diameter which is representative for most of the rem counter types. The scanning profiles along the X-axis are presented in Fig. 21 for neutron beam exposures in different

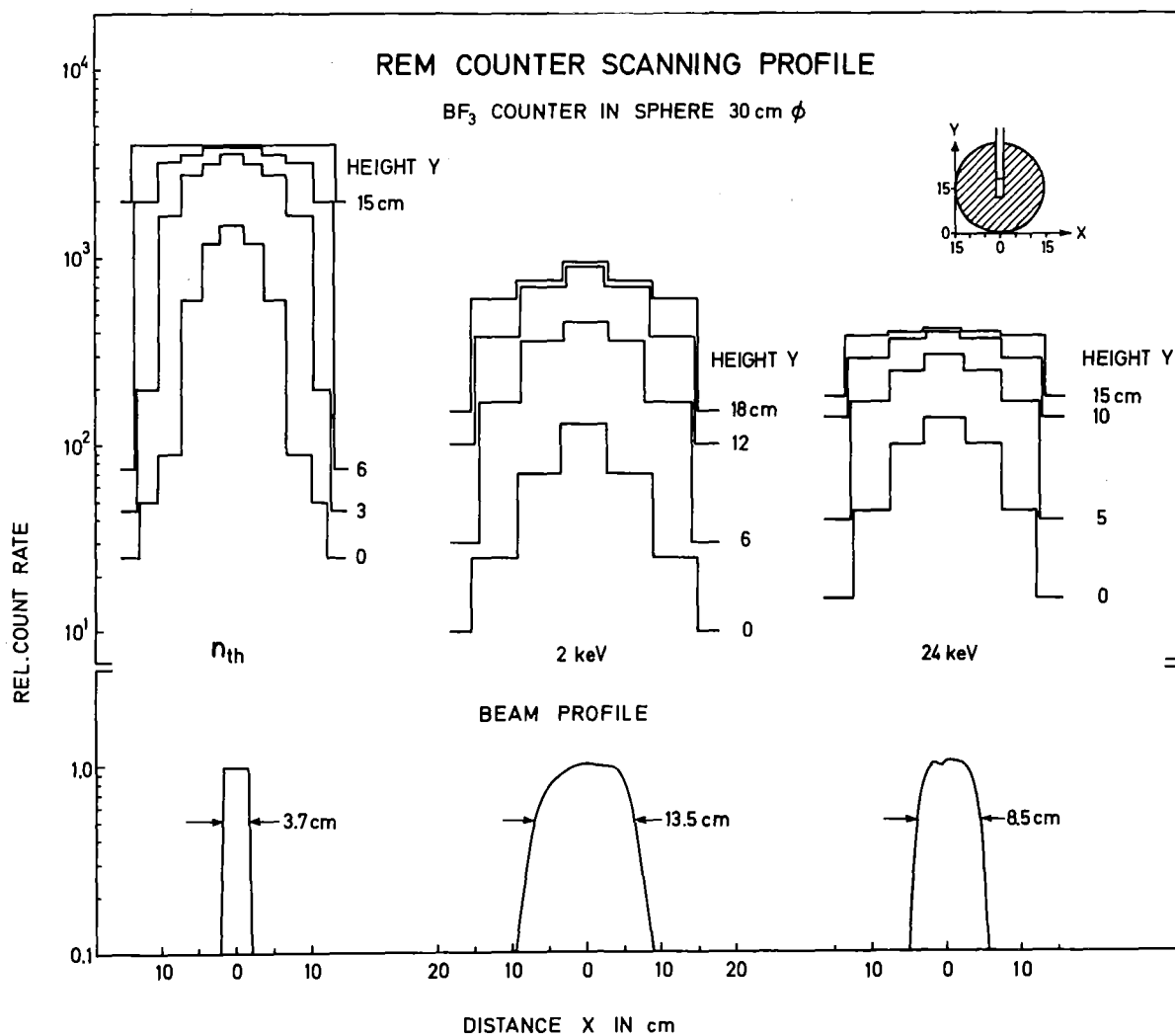


Fig. 21 Scanning profile of a rem counter with a BF_3 counter in the center of a polyethylene sphere of 30 cm diameter

distances from the center and are compared with the PTB beam profile for n_{th} , 2 keV and 24 keV neutrons. Compared to the central exposure with the thermal neutron beam of 3.7 cm diameter practically no change in the response was found up to distances of 11 cm from the center.

5.2 Detector on the Surface

The albedo counter makes use of three BF_3 counters positioned outside and behind the boron/plastic shield at the surface of a polyethylene cylinder. The BF_3 counters have been exposed in the position *i* facing the body, in position *m* inside the boron shield and in position *a* at the surface of the boron shield and the scanning profiles are presented in Fig. 22. In position *i* the central beam exposure with thermal neutrons results in a minimum count rate due to the boron shield. It can be seen from the figure that only a small area around the boron shield takes part to the moderation and the reflection of incident neutrons which are detected afterwards. Because of the location of position *m* in the moderator a count rate ratio $m/a > 1$ was found compared to $m/a = 1$ for the albedo dosimeter.

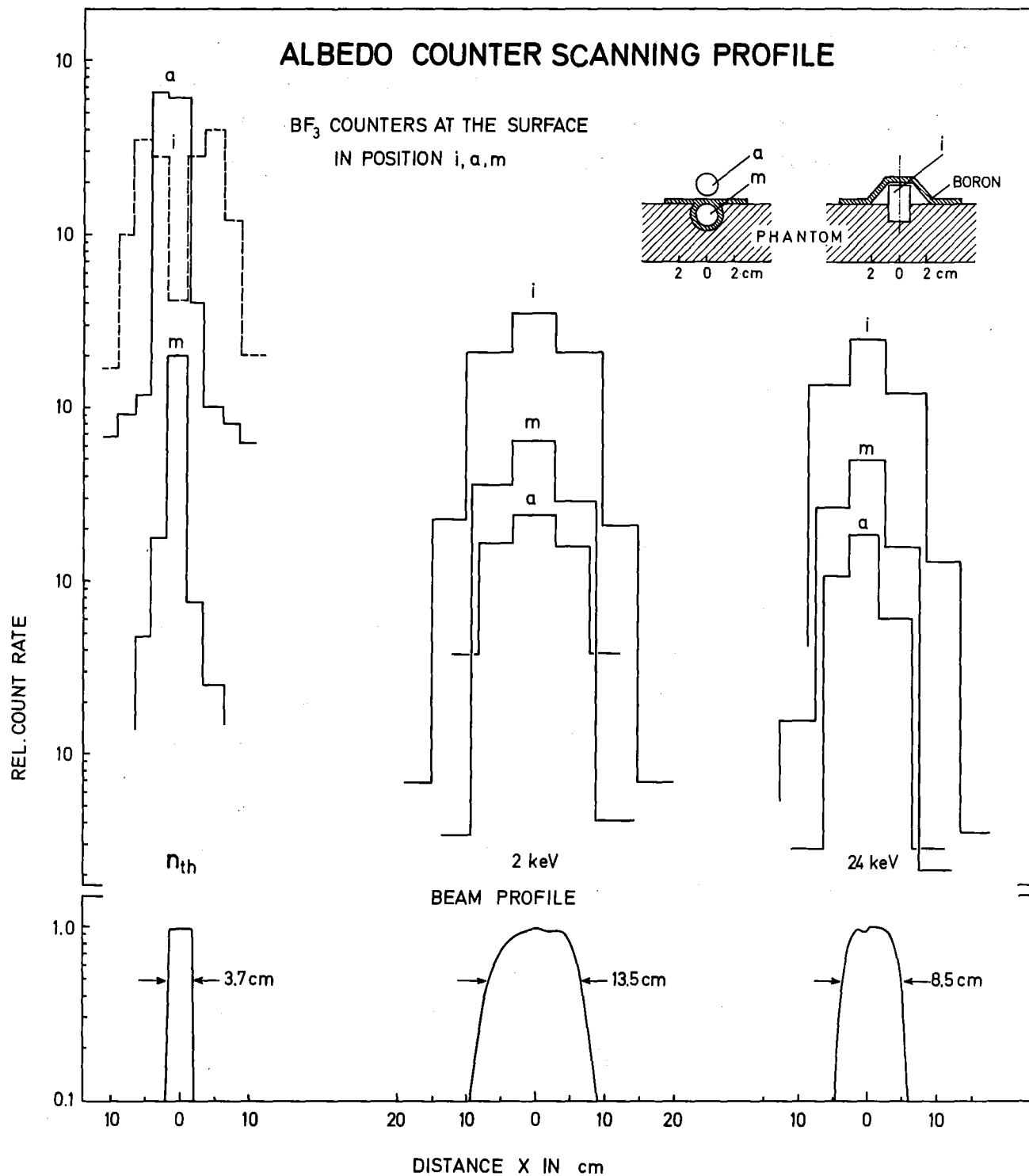


Fig. 22 Scanning profile of an albedo counter with three BF₃ counters in the position i, a, m, at the surface of a polyethylene cylinder

5.3 Detector Along the Beam Axis

The passive spectrometer with TLD 600/TLD 700 detectors along the central axis of the moderator cylinder of 25 cm diameter and height was irradiated with the thermal neutron beam of 3.5 cm diameter.

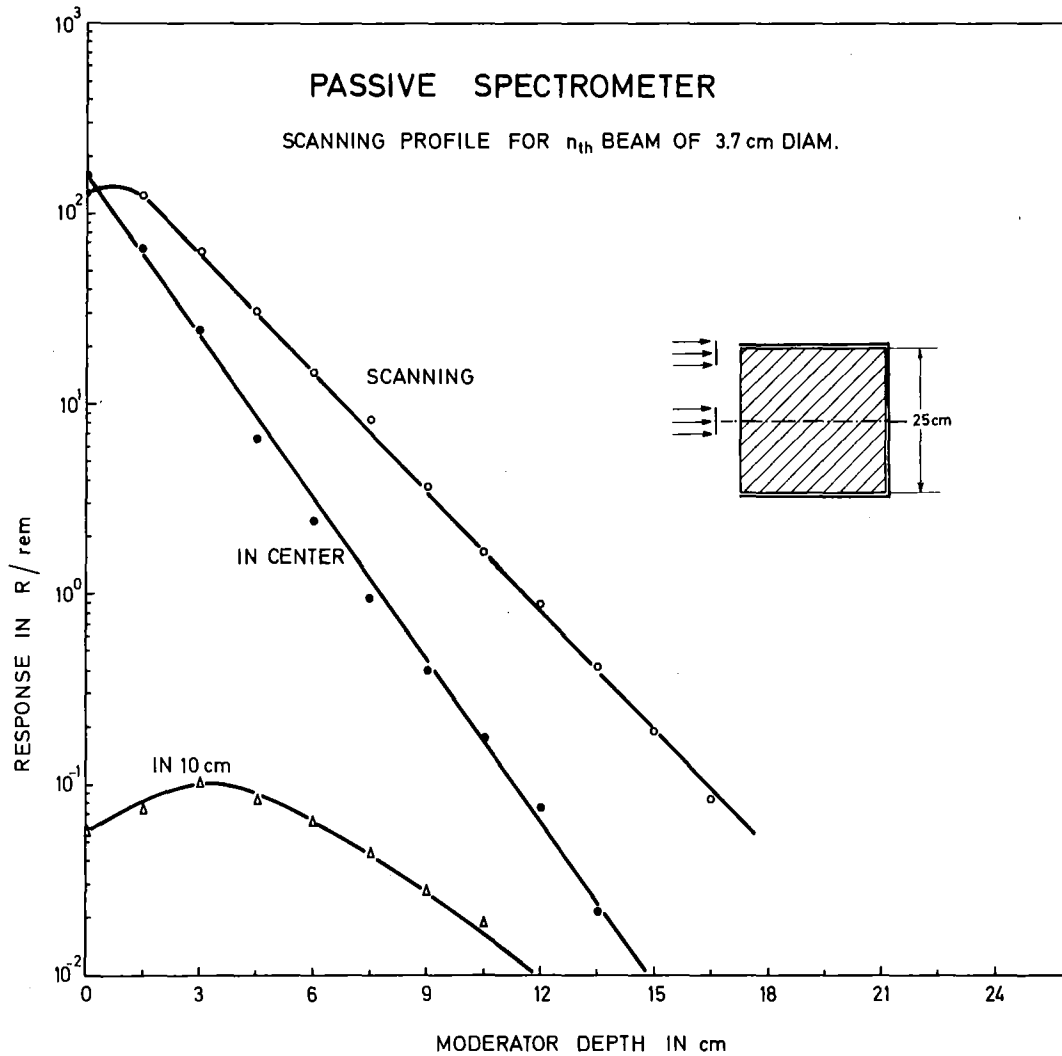


Fig. 23 Response vs. depth of TLD 600/TLD 700 detectors in the axis of the passive spectrometer for different beam exposures with thermal neutrons

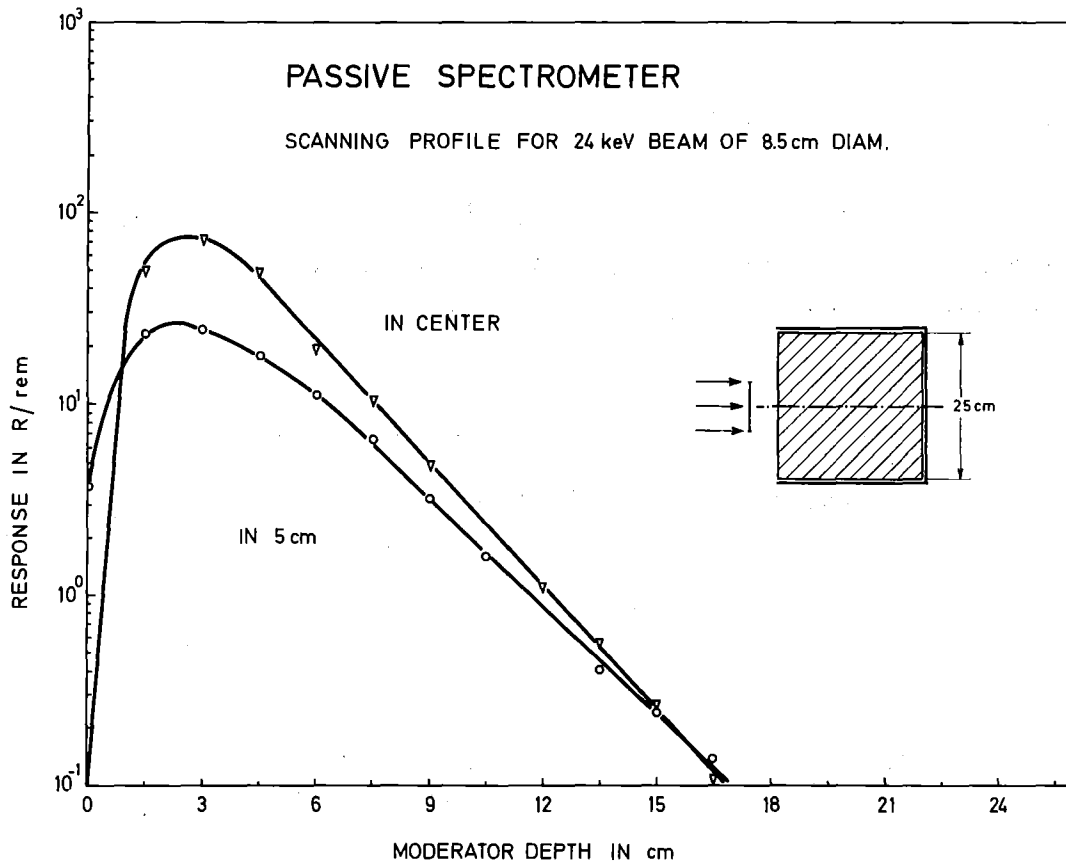


Fig. 24 Response vs. depth of TLD 600/TLD 700 detectors in the axis of the passive spectrometer for different beam exposures with 24 keV

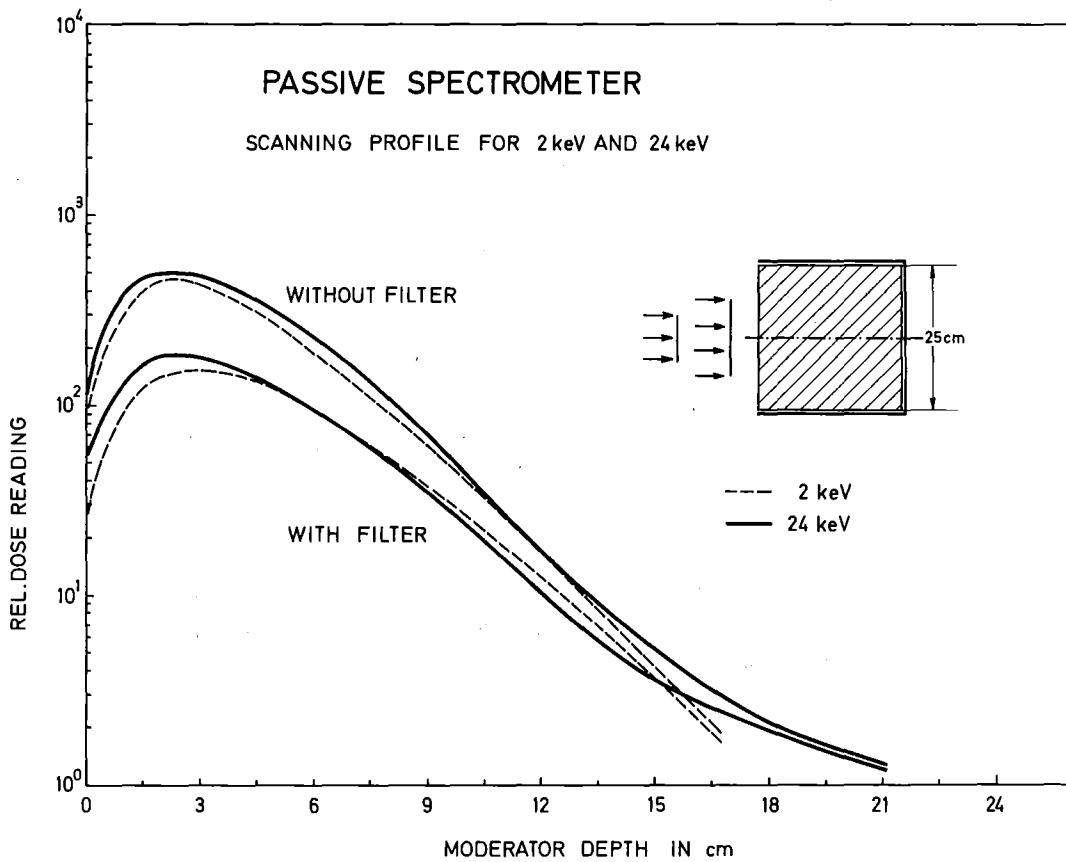


Fig. 25 Relative dose reading of TLD 600/TLD 700 detectors in the axis of the passive spectrometer vs. depth for a central beam of 2 keV and 24 keV neutrons with different filters

Fig. 23 shows the depth dose curves for different beam exposures to thermal neutrons. These are the exposure in the cylinder axis, the exposure in a distance of 10 cm from the center and the exposure over the total cross section of the cylinder. In a depth of 12 cm the gamma equivalent neutron dose reading per 1 rem was found to be 0.9 R/rem for the total exposure of the detector, 0.07 R/rem for a beam exposure along the axis and 0.01 R/rem in 10 cm distance from the center. Similar results found for 24 keV beam exposures are presented in Fig. 24.

The scanning profile for beam exposures with 2 keV and 24 keV presented in Fig. 25 results in the same increase in response as a function of moderator depth. On the basis of a depth dose curve analysis it is therefore not possible to interpret the neutron spectra in terms of effective neutron energy if the neutron energy is lower than 50 keV.

6. Interpretation of Neutron Spectra

On the basis of the response vs. depth curves of the passive spectrometer various parameters may be used for the estimation of relaxation length, effective energy of the neutron spectrum and the amount of backscattered thermal neutrons, for instance,

- the dosimeter reading R_0 at the surface of the polyethylene cylinder,
- the depth d_{\max} in polyethylene, where the maximum dosimeter reading R_{\max} occurs,
- the decrease in dose reading due to attenuation in polyethylene which follows the built-up of thermal neutrons in few cm.

As it was found experimentally the depth dose curve may be applied for a more or less quantitative interpretation of the neutron spectrum which, however, is restricted to neutron energies ranging from 50 keV to 5 MeV. The increase in the depth dose in the first tissue layers behind the surface as well as the maximum of the depth dose curves are characteristic parameters for an analysis of the neutron spectrum.

The results found with the passive spectrometer were applied to interpret the neutron spectra at the irradiation facilities at the PTB and the GSF. With respect to the calibration results found for 19 MeV neutrons it was supposed that the high energy beam obviously includes also an additional low energetic component. In Fig. 26 a trial was made to interpret the depth dose curve found for the 19 MeV irradiation. For a rough analysis of the 19 MeV spectra the difference of the depth dose curves for 19 MeV and 15.5 MeV resulted in a low energy component with $E_{\text{eff}} \leq 250$ keV. Taking into account the higher response at 250 keV the dose equivalent fraction of this neutron component is in the order of 14% and comparable with a low energy fluence of approximately 10% which was found experimentally at the PTB [29].

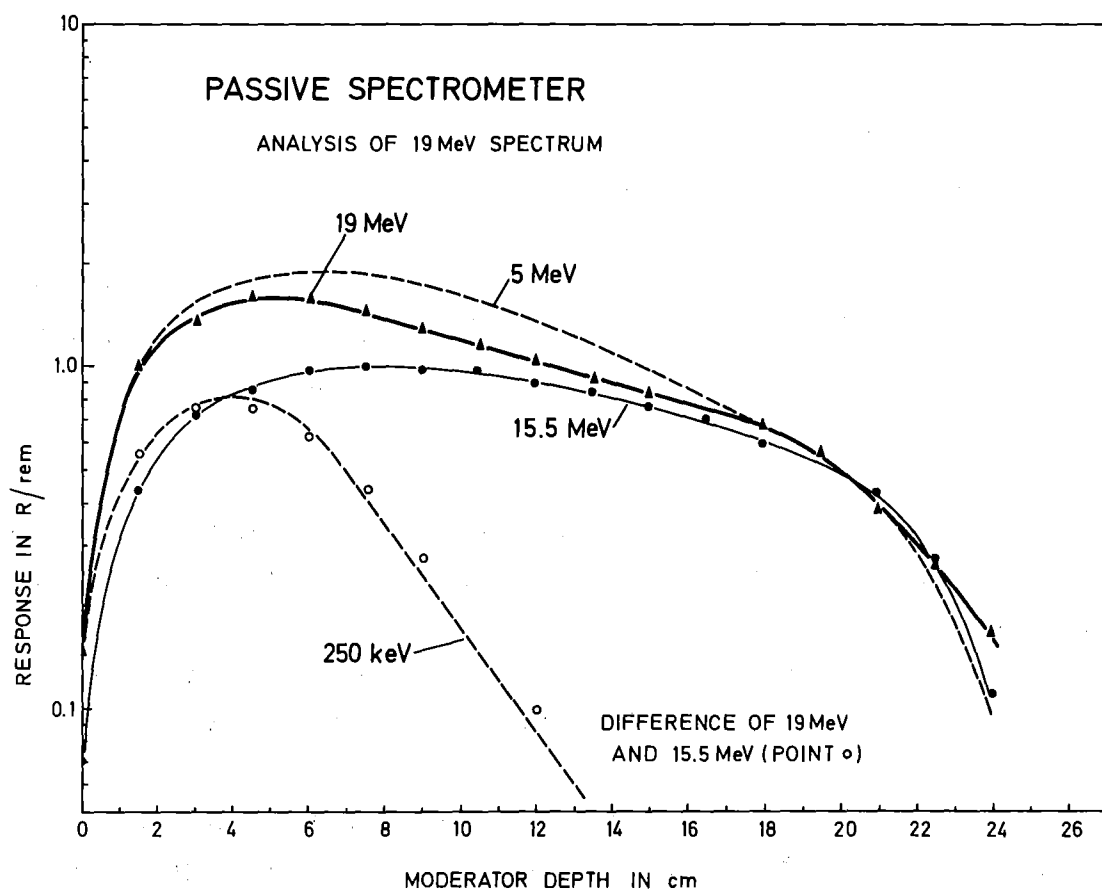


Fig. 26 Depth dose curves of TLD 600/TLD 700 detectors in the axis of the passive spectrometer vs. depth for a 19 MeV and 15.5 MeV neutron exposure at the PTB and analysis of a low energy component

For the irradiation at PTB and GSF the same neutron energies of 570 keV, 5 MeV and 15.5 MeV have been used. On the basis of passive spectrometer results it was of general interest to compare the neutron spectra as well as the response of the spectrometer for both calibration exposures.

It can be seen from Fig. 26 that all depth dose curves are identical in shape representing an excellent agreement in the beam quality as well as in the absolute response for the TLD 600/TLD 700 detector. The 15 MeV beam calibrations at PTB and GSF agree within $\pm 5\%$, an excellent result with respect to the different methods of beam calibration at PTB and GSF. On the basis of the response curves the agreement in the calibration of the other beams is better than $\pm 1.5\%$. This accuracy which was found for the interpretation of neutron spectra is surprising because the error sources for the evaluation of a single TLD is in the order of 3%. By fitting the depth dose curve the total error will be obviously reduced.

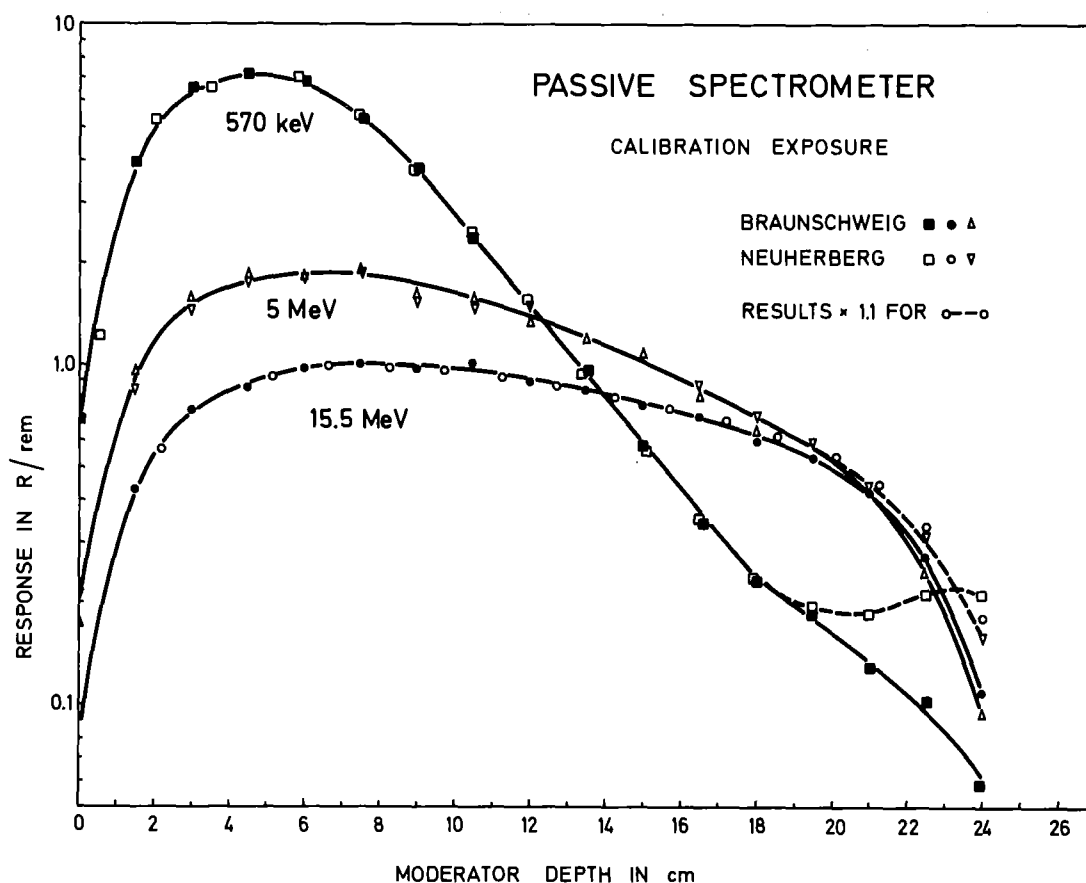


Fig. 27 Depth dose curves of TLD 600/TLD 700 detection in the axis of the passive spectrometer vs. depth for the irradiations at the PTB and GSF with 570 keV, 5 MeV and 15.5 MeV neutrons

Acknowledgements

The authors wish to thank the Commission of the European Communities, above all Mr. H. Seguin from the Health and Safety Directorate and Dr. S. Wagner from the PTB Braunschweig for the organization of the neutron workshop. The results of this workshop are of high actuality and will stimulate further activities in neutron dosimetry.

We are grateful to Dr. W. G. Alberts, Dr. M. Cosack, Mr. H. Kluge, Dr. Zill from the PTB Braunschweig and Dr. H. Schraube from the GSF Neuherberg for the collaboration and discussions during the experiments.

It is a pleasure to acknowledge the cooperation of the staff of the irradiation facilities of the Physikalisch-Technische Bundesanstalt Braunschweig during the calibration experiments.

7. References

- [1] Alberts, W.G., et al., Proc. IAEA Symposium on Advances in Radiation Protection Monitoring, Stockholm, 1978
- [2] Coseck, M., et al., Proc. Euratom Symposium on Neutron Dosimetry in Biol. and Medic., EUR 4896 I, 1972, p. 267
- [3] Barne, S.J., et al., Rev. Sci. Instr. 28, 1957, p. 997
- [4] Schraube, H., Burger, G., Seguin, H., Proc. IAEA Symposium on Advances in Radiation Protection Monitoring, Stockholm, 1978
- [5] Broerse, J.J., Burger, G., Coppola, M., Eds., EUR 6004, 1978
- [6] Alberts, W.G., et al., "Euratom Workshop on Neutron Dosimetry for Radiation Protection", PTB report to be published, 1979
- [7] Singh, D., Burgkhardt, B., Piesch, E., Nucl. Instr. Meth. 142, 1977, p. 409
- [8] Burgkhardt, B., Piesch, E., Schmitt, A., in Report KfK 2620, 1978, p. 85
- [9] Piesch, E., Burgkhardt, B., Proc. 4th Int. Conf. Lum. Dosimetry, Krakow, 1974, p. 1123
- [10] Piesch, E., Burgkhardt, B., Proc. IAEA Symposium on Advances in Radiation Protection Monitoring, Stockholm, 1978
- [11] Burgkhardt, B., et al., Nucl. Instr. Meth. 160, 1979, p. 533
- [12] Alsmiller, R.G., Barish, J., Health Physics 26 1974, p. 13

- [13] Nollmann, C., Burgkhardt, B., Piesch, E., Nucl. Instr. Meth. 161, 1979, p. 449
- [14] Hoy, J., Proc. 6th ERDA Workshop Person. Neutr. Dosim., PNL-2449, 1977, p. 96
- [15] Hankins, D.E., Report LA-4832 (1972) and in report PNL-2449, 1977, p. 67
- [16] Burgkhardt, B., Piesch, E., Schmid, S., Vortrag 10. wiss. Jahrestagung Deutsche Ges. f. Mediz. Physik, Braunschweig, 1979
- [17] Burgkhardt, B., Krauss, O., Piesch, E., Vortrag 10. wiss. Jahrestagung Deutsche Ges. f. Mediz. Physik, Braunschweig, 1979
- [18] Borchardt, D., Kirschfeld, K., Hahn-Meitner-Institut Berlin, private communication, 1978, see also [6]
- [19] Cross, W.G., Tommasino, L., Rad. Eff. 5, 1970, p. 85
- [20] Hassib, G.M., Kasim, S.A., Piesch, E., to be published 1979
- [21] Hassib, G.M., Nucl. Tracks, 3, 1979, p. 45
- [22] Hassib, G.M., Piesch, E., 7th DOE Workshop Pers. Neutr. Dosimetry, London, PNL-2807, 1978, p. 71
- [23] Griffith, R.V., Fischer, J.C., Harder, C.A., UCRL-50007-76-1, 1976, p. 40
- [24] Jozefowicz, K., Proc. IAEA Symposium Neutr. Monit., Vienna, Vol. II, 1973, p. 183
- [25] Piesch, E., Atompraxis, 1963, p. 179
- [26] Piesch, E., Sayed, M.A., Nucl. Instr. Meth. 123, 1975, p. 397

- [27] Bartlett, D.T., 7th DOE Workshop Pers. Neutr. Dosim., London, PNL-2807, 1978, p. 46

- [28] Amadesi, P., Cavallini, A., *Minerva Nucleare*, 5, No. 12, 1961, p. 323

- [29] Coseck, M., paper presented at the Euratom Seminar on Neutron Dosimetry, Berkeley, UK, 1978

- [30] Piesch, E., Proc. IAEA Symposium Neutr. Monit., Vienna, 1966, p. 471

- [31] Harrison, K.G., to be published, 1979

Figure Captions

- Fig. 1 Cross section of the neutron spectrometer (a) and the dosimeter (b) with cylindrical shape
- Fig. 2 Gamma equivalent neutron dose reading of TLD 600/TLD 700 dosimeters in Roentgen per neutron dose equivalent of 1 rem as a function of depth in beam axis
- Fig. 3 Neutron response of the passive spectrometer with TLD 600/TLD 700 detectors along the cylinder axis as a function of depth
- Fig. 4 Ratio of response in 12 cm depth and in the maximum of depth dose curve vs. neutron energy
- Fig. 5 Response vs. neutron energy for the Studsvik rem counter and a rem counter with a BF_3 counter in the center of a sphere of 30 cm diameter
- Fig. 6 Response vs. neutron energy for passive rem counters with TLD 600/TLD 700 in the center of a moderator
- Fig. 7 Response vs. neutron energy of the Karlsruhe albedo dosimeter and an albedo counter with BF_3 detectors
- Fig. 8 Energy dependence of the Karlsruhe albedo dosimeter for TLD 600/TLD 700 in position i compared with calculated data
- Fig. 9 Detector reading ratio of the Karlsruhe albedo dosimeter vs. neutron energy
- Fig. 10 Directional dependence vs. neutron energy for the Karlsruhe albedo dosimeter

- Fig. 11 Response of the albedo detector i as a function of detector ratio i/a with H_{th}/H and E as parameters
- Fig. 12 Calibration factor of albedo detectors compared to the reading ratio 9"/2" and 12"/2" spheres vs. neutron energy
- Fig. 13 Comparison of measured and calculated reading ratio of 12"/2" spheres
- Fig. 14 Energy dependence of ^{237}Np fission fragment track etch detector vs. neutron energy and the ^{237}Np (n,f) cross section
- Fig. 15 Energy dependence of ^{232}Th fission fragment track etch detector vs. neutron energy and the ^{232}Th (n,f) cross section
- Fig. 16 Response of the Kodak LR-115 film applied as recoil track etch detector vs. neutron energy
- Fig. 17 Response vs. neutron energy of Makrofol E recoil track etch detector after electrochemical etching
- Fig. 18 Measured and calculated response vs. neutron energy of the Kodak NTA film emulsion sealed in aluminium/plastic foil
- Fig. 19 Response vs. number of tracks of the NTA film for free air and phantom exposures
- Fig. 20 Energy dependence of phosphate glass dosimeters
- Fig. 21 Scanning profile of a rem counter with a BF_3 counter in the center of a polyethylene sphere of 30 cm diameter
- Fig. 22 Scanning profile of an albedo counter with three BF_3 counters in the position i, a, m , at the surface of a polyethylene cylinder

- Fig. 23 Response vs. depth of TLD 600/TLD 700 detectors in the axis of the passive spectrometer for different beam exposures with thermal neutrons
- Fig. 24 Response vs. depth of TLD 600/TLD 700 detectors in the axis of the passive spectrometer for different beam exposures with 24 keV
- Fig. 25 Relative dose reading of TLD 600/TLD 700 detectors in the axis of the passive spectrometer vs. depth for a central beam of 2 keV and 24 keV neutrons with different filters
- Fig. 26 Depth dose curves of TLD 600/TLD 700 detectors in the axis of the passive spectrometer vs. depth for a 19 MeV and 15.5 MeV neutron exposure at the PTB and analysis of a low energy component
- Fig. 27 Depth dose curves of TLD 600/TLD 700 detection in the axis of the passive spectrometer vs. depth for the irradiations at the PTB and GSF with 570 keV, 5 MeV and 15.5 MeV neutrons